Late Holocene earthquakes on the Toe Jam Hill fault, Seattle fault zone, Bainbridge Island, Washington

Alan R. Nelson†
Samuel Y. Johnson
Geologic Hazards Team, U.S. Geological Survey, MS 966, P.O. Box 25046, Denver, Colorado 80225, USA

Harvey M. Kelsey
Department of Geology, Humboldt State University, Arcata, California 95521, USA

Ray E. Wells
Western Regional Geology Team, U.S. Geological Survey, MS 975, 345 Middlefield Road, Menlo Park, California 94025, USA

Brian L. Sherrod
U.S. Geological Survey at Department of Earth and Space Sciences, Box 351310, University of Washington, Seattle, Washington 98195, USA

Silvio K. Pezzopane
Water Resources Division, U.S. Geological Survey, MS 421, P.O. Box 25046, Denver, Colorado 80225, USA

Lee-Ann Bradley
Geologic Hazards Team, U.S. Geological Survey, MS 966, P.O. Box 25046, Denver, Colorado 80225, USA

Rich D. Koehler III
William Lettis and Associates, Inc., 999 Andersen Drive, Suite 120, San Rafael, California 94901, USA

Robert C. Bucknam
Geologic Hazards Team, U.S. Geological Survey, MS 966, P.O. Box 25046, Denver, Colorado 80225, USA

ABSTRACT

Five trenches across a Holocene fault scarp yield the first radiocarbon-measured earthquake recurrence intervals for a crustal fault in western Washington. The scarp, the first to be revealed by laser imagery, marks the Toe Jam Hill fault, a north-dipping backthrust to the Seattle fault. Folded and faulted strata, liquefaction features, and forest soil A horizons buried by hanging-wall-collapse colluvium record three, or possibly four, earthquakes between 2500 and 1000 yr ago. The most recent earthquake is probably the 1050–1020 cal. (calibrated) yr B.P. (A.D. 900–930) earthquake that raised marine terraces and triggered a tsunami in Puget Sound. Vertical deformation estimated from stratigraphic and surface offsets at trench sites suggests late Holocene earthquake magnitudes near M7, corresponding to surface ruptures >36 km long. Deformation features recording poorly understood latest Pleistocene earthquakes suggest that they were smaller than late Holocene earthquakes. Postglacial earthquake recurrence intervals based on 97 radiocarbon ages, most on detrital charcoal, range from ~12,000 yr to as little as a century or less; corresponding fault-slip rates are 0.2 mm/yr for the past 16,000 yr and 2 mm/yr for the past 2500 yr. Because the Toe Jam Hill fault is a backthrust to the Seattle fault, it may not have ruptured during every earthquake on the Seattle fault. But the earthquake history of the Toe Jam Hill fault is at least a partial proxy for the history of the rest of the Seattle fault zone.

Keywords: paleoseismology, earthquake recurrence, reverse faulting, Puget Lowland, fault trenching, earthquake hazards.

INTRODUCTION

With a history of one documented large earthquake 1100 yr ago (Bucknam et al., 1992; Sherrod et al., 2000), the Seattle fault zone—an east-west belt of young thrusts traversing the Puget Lowland (Fig. 1)—presents a poorly known earthquake hazard. Like crustal faults in some other well-populated basins (e.g., Dolan et al., 1995; Sugiyama, 2000), the thrusts may pose a greater hazard than do much longer but more distant plate-boundary faults. Efforts to quantify the earthquake hazard in the Puget Lowland (Frankel et al., 2002) are hampered by the absence of earthquake recurrence intervals for any lowland crustal faults. Here, through study of the earthquake history of a surface-rupturing backthrust in the Seattle fault zone, we report the first radiocarbon-measured recurrence intervals for a fault in the Puget Lowland. The intervals define a cluster of earthquakes in the late Holocene, preceded by many thousands of years of postglacial quiescence.

†E-mail: anelson@usgs.gov.

GSA Bulletin; November 2003; v. 115; no. 11; p. 1388–1403; 7 figures; 1 table; Data Repository item 2003151.

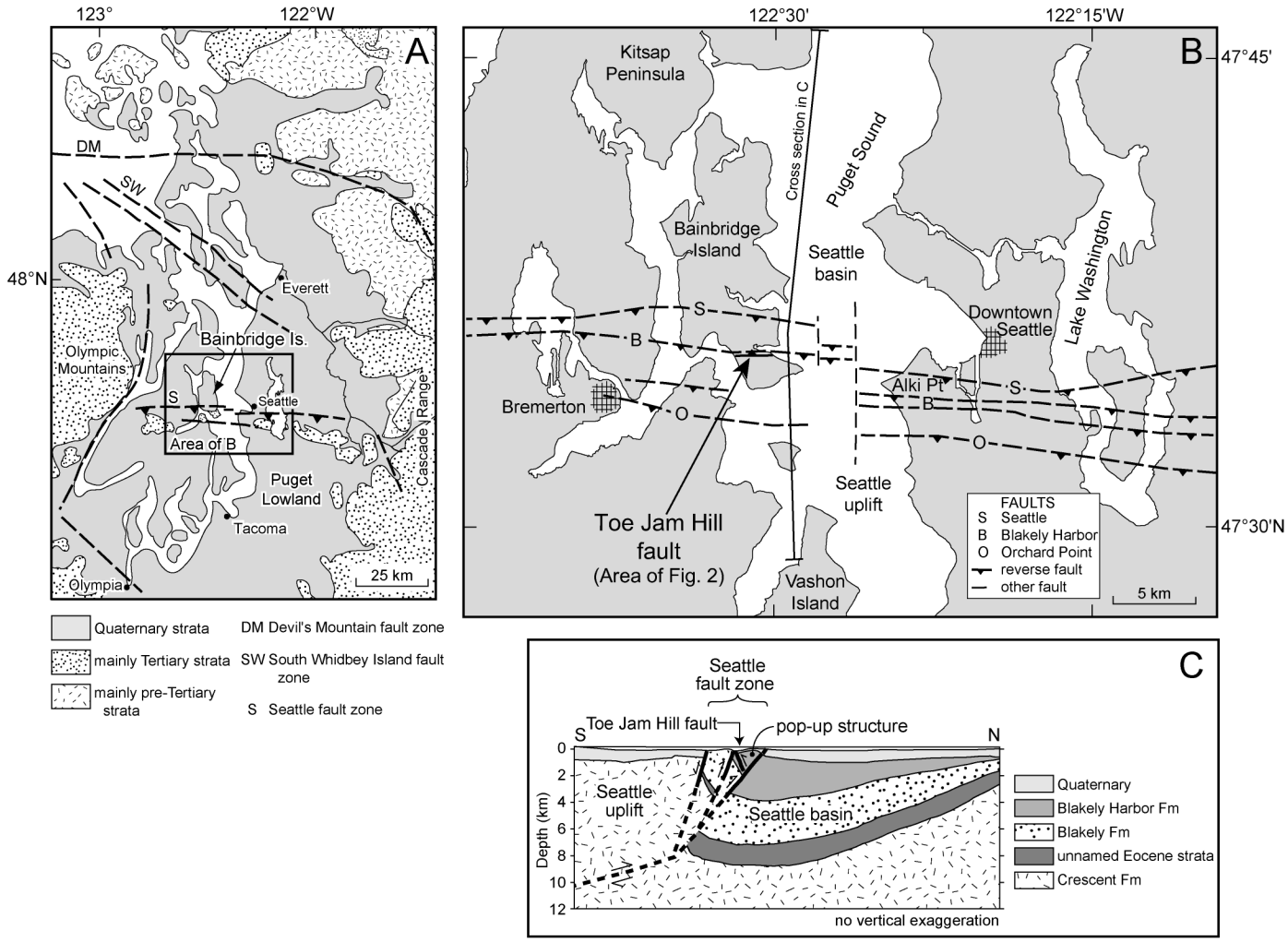

Figure 1. (A) Geologic map of the Puget Lowland region showing location of Bainbridge Island and selected regional crustal fault zones (dashed lines; after Bourgeois and Johnson, 2001). (B) Map showing principal reverse faults and tear faults of the Seattle fault zone in central Puget Sound and the location of the Toe Jam Hill fault on southern Bainbridge Island (Johnson et al., 1999; Blakely et al., 2002). (C) North-south cross section through Bainbridge Island (cross-section location in B) showing probable structural relationships among the Toe Jam Hill fault and other faults of the Seattle fault zone.

Holocene faulting and folding were widely suspected but undocumented in the Puget Lowland (Gower et al., 1985) until abundant shorelines and their deposits were recognized as potential archives of prehistoric earthquakes (e.g., Bucknam et al., 1992; Atwater and Moore, 1992). Today, shoreline studies are complemented by the application of airborne laser swath mapping (ALSM)—a tool that reveals previously unknown Holocene fault scarps beneath the forest canopy (Fig. 2; Bucknam et al., 1999; Harding and Berghoff, 2000; Haugerud et al., 2003). Our study of five trenches on Bainbridge Island, dug across the first laser-revealed fault scarp in the lowland (Figs. 1 and 2), is the second trench study on young scarps in western Washington (following the pioneering work of Wilson et al., 1979) and the first to yield abundant ^{14}C ages.

SEATTLE FAULT ZONE

The Seattle fault zone—spanning ~70 km from the Cascade Range foothills to Hood Canal (Fig. 1)—is one of several fault zones in the Puget Lowland that help accommodate the 4–7 mm/yr of north-south shortening resulting from northward migration of the forearc of the Cascadia convergent margin (Fig. 1; Wells et al., 1998; Miller et al., 2001; Mazzotti et al., 2002; Hyndman et al., 2003). The Seattle fault zone has been imaged on seismic reflection profiles in Puget Sound and adjacent waterways (Johnson et al., 1994, 1999; Pratt et al., 1997; ten Brink et al., 2002), correlates with large gravity and magnetic anomalies (Blakely et al., 2002), and is marked by a prominent velocity anomaly on tomographic models (Brocher et al., 2001; Calvert et al., 2001). At least three south-dipping thrusts—the Seattle fault (the frontal fault of Blakely et al., 2002), the Blakely Harbor fault, and the Orchard Point fault (Blakely et al., 2002)—inferred from these data and geologic mapping (e.g., Haeussler et al., 2000) comprise the Seattle fault zone, which forms the structural boundary between uplifted Tertiary rocks of the Seattle uplift on the south and thick Tertiary to Quaternary strata of the Seattle basin on the north (Fig. 1C).

In this paper we focus on a 2-km-long back-

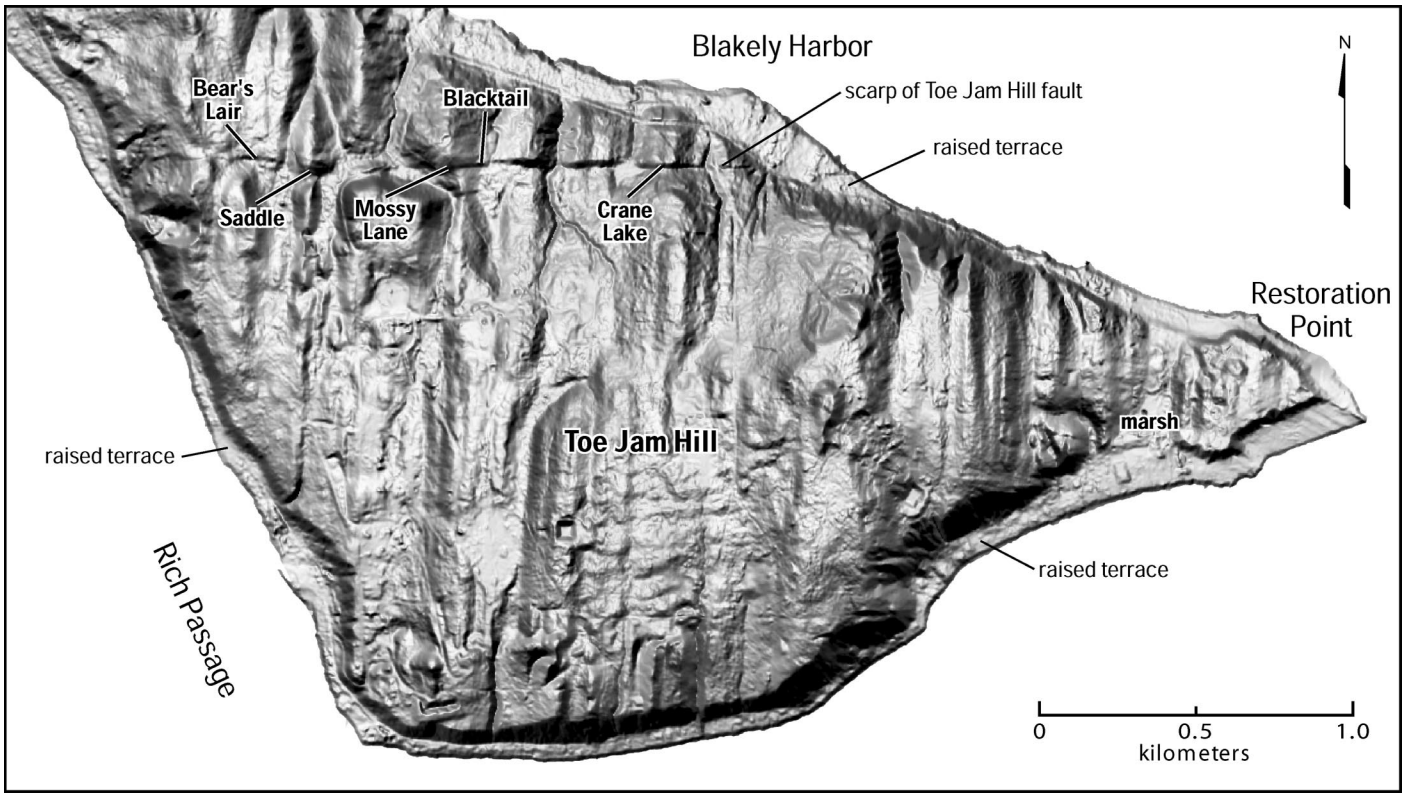

Figure 2. Airborne laser swath mapping (ALSM) digital elevation model of the southernmost part of Bainbridge Island, Washington (location in Fig. 1B; model grid cells are 3.7 m square). The south-facing scarp of the Toe Jam Hill fault trends east-west across the island ~200–500 m south of Blakely Harbor. Leaders locate the five trench sites along the scarp. A 1:2500-scale figure showing trench and scarp-profile locations appears in Nelson et al. (2002). Raised marine terraces studied by Bucknam et al. (1992) and Harding et al. (2002) and the marsh west of Restoration Point studied by Sherrod et al. (2000) are labeled.

thrust on Bainbridge Island that dips north into the Seattle fault, probably forming a pop-up structure on its hanging wall (Fig. 1; McClay, 1992; Blakely et al., 2002). We name the backthrust the ''Toe Jam Hill fault'' after a hill that crests ~1 km south of the fault's east-west scarp (Fig. 2). Seismic reflection and refraction studies and geologic mapping of the Seattle fault imply dips of 40°–70°S in the upper 5–6 km of crust with shallower dips of ~20°–30°S at greater depths (Pratt et al., 1997; Johnson et al., 1994, 1999; Haeussler et al., 2000; ten Brink et al., 2002). Elastic models of Seattle fault slip using reflection, velocity, gravity, and shoreline-uplift data incorporate a pop-up block bounded by shallow faults in the hanging wall of the Seattle fault (ten Brink et al., 2002), and Blakely et al. (2002, their Fig. 5D) similarly included a pop-up in one of their two alternative models for the structure of the Seattle fault zone. Such pop-ups at meter to kilometer scales are common features of young reverse-faulting terrains (Bilham and Yu, 2000; Kelson et al., 2001). The microseismicity-based structural model of Brocher et al. (2001, their Plate 8) and the alternative model of Blakely et al. (2002, their Fig. 5C) yield much steeper dips of ~80°S for the Seattle fault. Because the Toe Jam Hill fault must merge with the Seattle fault above seismogenic depths (~10 km) unless the dips on both faults exceed 84°, we favor the pop-up model whereby the Toe Jam Hill fault is antithetic to, and so does not rupture independently from, the Seattle fault. If the pop-up model is correct, the history of the Toe Jam Hill fault may be an incomplete proxy for the history of the Seattle fault. Slip on the Seattle fault might not always activate the Toe Jam Hill fault, but every surface deformation event on the Toe Jam Hill fault requires slip on the Seattle fault.

Coastal geology documents a large prehistoric earthquake in the Seattle fault zone. First identified from a coseismically raised marine terrace 5–7 m high at Restoration Point (Fig. 2), uplift extends 5–10 km southward from the Seattle fault and 30 km eastward from Bremerton to Seattle (Fig. 1B; Bucknam et al., 1992; Harding et al., 2002). The earthquake dates from 1050–1020 cal. yr B.P. (A.D. 900–930) on the basis of multiple, high-precision ^{14}C ages on a log buried in a sand sheet deposited by the earthquake's tsunami at West Point near Seattle (Atwater and Moore, 1992; Atwater, 1999). Other temporally correlated earthquake effects in the lowland include tsunamis, subsidence, and intertidal liquefaction near Everett in the north-central Puget Lowland (Bourgeois and Johnson, 2001), lake turbidites and shoreline erosion in Lake Washington (Karlin and Abella, 1996; Thorson, 2000a), and intertidal uplift and subsidence in the southern Puget Lowland (Bucknam et al., 1992; Sherrod, 2001).

APPROACH

Scarp Trenching

The scarp of the Toe Jam Hill fault, the most distinct fault scarp in the Seattle fault zone, truncates the north-south grain of the glaciated landscape of southernmost Bainbridge Island a few hundred meters south of

Blakely Harbor (Fig. 2). The south-facing, 2.6-km-long scarp was identified in 1997 on a shaded digital elevation model made from ALSM data. Scarp height decreases from between 3 and 6 m in its central section to <1.5 m near either end. Trench stratigraphy shows that the scarp largely postdates the recession of the Puget Lobe glacier from the central Puget Lowland at ca. 16 ka (ka, thousand years before A.D. 1950) (Porter and Swanson, 1998). Gentle facets on topographic profiles across the scarp (Nelson et al., 2002) probably reflect irregular hanging-wall folding like that observed following historic reverse-faulting earthquakes (e.g., Philip et al., 1992; Bilham and Yu, 2000; Kelson et al., 2001).

Five 15–32-m-long trenches excavated along a 1.6-km-long section of the scarp revealed differences in stratigraphy and styles of faulting and folding (Figs. 2–5). Trenches on ridges where the scarp is highest (2.9–5.4 m; Saddle, Mossy Lane, and Crane Lake sites, Fig. 2) expose highly weathered mudstone and sandstone of the Miocene Blakely Harbor Formation mantled by patches of thin, root-stirred drift. Ridge trenches show weathered mudstone and Holocene colluvium thrust over younger colluvium and organic-rich, soil A-horizon sediment. Multiple near-vertical reverse faults in the Crane Lake trench (Fig. 5) contrast with the 30°-dipping Holocene thrust in the Saddle trench (Fig. 4B) and with five subhorizontal thrusts in the upper part of the Mossy Lane trench (Fig. 4A). At the Bear's Lair and Blacktail sites, excavated in glacial grooves where low scarps (2.1–3.6 m) dam north-flowing streams to form wetlands, trenches exposed folded till, outwash, ice-contact drift, and proglacial lake deposits overlain by Holocene lake and wetland deposits (Fig. 3). The fault responsible for folding the sediments is not exposed in the Blacktail trench. A 1-m-wide, graben-like fissure in the Bear's Lair trench documents coseismic extension during or after folding. In all trenches, ubiquitous root-stirring has obscured stratigraphic relationships to depths of 0.3–0.5 m. Although three of five small stream valleys that cut the scarp appear offset right laterally less than a few tens of meters, slickensides and other trench data do not suggest significant lateral fault slip. Complete trench logs; descriptions and interpretations of stratigraphic units; tables of lithologic, radiocarbon, soil profile, and paleoecologic data; and descriptions of data-collection methods and references are presented in Nelson et al. (2002).

Dating

We dated stratigraphic units through ^{14}C analysis; most ages came from accelerator mass spectrometer (AMS) analysis of unabraded fragments of wood charcoal (Table DR1[1]; complete data in Nelson et al., 2002). Of the 97 ages, 7 were by liquid scintillation counting on multigram pieces of wood or charcoal. We picked two-thirds of the dated fragments directly from moist sediment collected from the trench wall; fragments in the remaining 36 samples appeared on 1 mm and/or 0.5 mm sieves following wet sieving of bulk sediment samples (50–800 g of sediment). For each dated sample, we selected the largest, most angular, least decayed fragments of charcoal, wood, and/or herb parts to minimize the chance of analyzing reworked carbon much older than the host sediment. Although fragments with root-like morphology were avoided, as many as seven noncharcoal samples with much younger-than-expected ages are probably decayed roots. Ages younger than 20 ka are calibrated to account for fluctuations in the rate of atmospheric ^{14}C production over time (Stuiver et al., 1998; Bronk Ramsey, 1998).

We qualitatively assessed those ages that might be much older or younger than their host sediment by evaluating the size and condition (decayed, abraded) of dated fragments and their stratigraphic consistency within and among correlative units. Comparisons of ages within each trench and among trenches suggest that 28 of the 97 ages differ by more than a few hundred years from the time that their host sediment was deposited—two-thirds of these (18) are too old and, therefore, are assumed to have been reworked (half-filled triangles in Figs. 3, 4, and 5).

The ten ages that are obviously too young in comparison with other ages (open triangles in Figs. 3, 4, and 5) fall into two cases: (1) fragments of decayed or burned roots that intruded down into host sediment, or (2) fragments incorporated into fractures or root casts that are no longer identifiable because of decay of soil organic material or root stirring. A test of case 1 in the Saddle trench yielded a 1.8 ka age on a burned oval-shaped tree root intruded into an older Holocene root cast in drift (Fig. 4B). Other drift units in this and the Blacktail trench (Fig. 3A) contain charcoal and decayed wood many thousands of years younger than the units' times of deposition. Case 2 is illustrated by three sets of paired ages (two from Bear's Lair and one from Blacktail) on fragments picked from the same bulk samples (0.5 mm sieve) of Holocene lake sediment: decayed fragments of root sheaths and leaves gave greater than modern ages, whereas angular fragments of charcoal gave ages of 9.6–7.5 ka (Table DR1 [see footnote 1]). Similar discordant-age pairs were obtained from samples of buried A-horizon and root-cast sediment in the Mossy Lane and Saddle trenches (Fig. 4). For most discordant-age pairs, the charcoal ages are closer to the time of host sediment deposition than the youngest ages.

An important issue in using detrital charcoal ages to date earthquakes is the average age of charcoal fragments on and within a forest soil. A study of soil charcoal by Gavin (2000, 2001) showed that ^{14}C-dated charcoal from the surface of soils in the old-growth forests of Vancouver Island was almost always <600 yr older than the time of the most recent forest fire and usually <400 yr older. From these data and the consistency in our ^{14}C ages from pieces of wood charcoal tens of millimeters thick picked from buried former forest floors (e.g., Figs. 4A and 5), we infer that large pieces at the tops of buried A horizons in the Toe Jam Hill fault trenches were rarely >500 yr old when buried by faulting. Gavin (2000, p. 66) also found that charcoal from the shallowest depths in forest soils consistently gave the youngest ages, particularly on hillslopes where most soil charcoal ages were <1000 yr older than the most recent fire. If fires have been frequent (e.g., Hemstrom and Franklin, 1982) and surface charcoal in Bainbridge Island forest soils is stirred into scarp (hillslope) soils within hundreds of years of the fires that produced it, then most large (>5-mm-diameter), angular fragments of charcoal from the upper ~0.5 m of buried soils are unlikely to be more than 1000–1500 yr older than the time of soil burial. This inference is supported by the younger than 1.3 ka ages on 14 of 17 samples of charcoal fragments at <0.5 m depth in Holocene colluvium in the trenches; only 2 of 24 ages on fragments >5 mm are >1500 yr older than our inferred times of soil burial.

Because soil relative-dating studies at low elevations elsewhere in the Puget Sound region (Dethier, 1988; Garcia, 1996) focused on soils developed on deposits much sandier than those in the Toe Jam Hill fault trenches, comparison of the characteristics of the sandy soils with those of clayey trench soils helps little in estimating trench soil ages. However, descriptions of 12 soil profiles and laboratory analysis of horizon samples (methods of Birkeland, 1999) in and near the trenches (Nelson et al., 2002) help us to identify periods of

[1]GSA Data Repository item 2003151, Table DR1, ^{14}C ages used to constrain times of deformation events, is available on the Web at http://www.geosociety.org/pubs/ft2003.htm. Requests may also be sent to editing@geosociety.org.

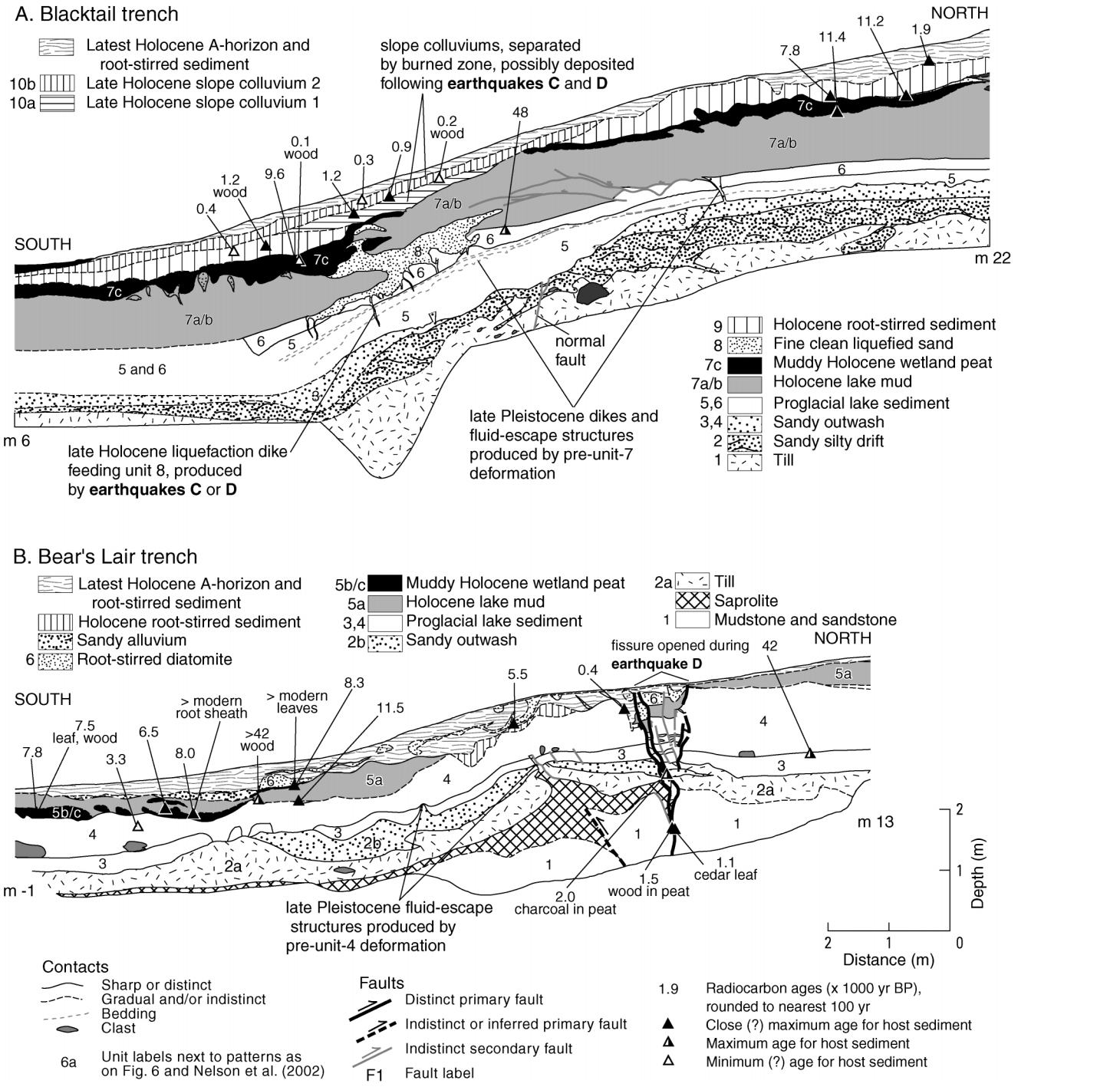

Figure 3. Simplified stratigraphy of (A) the central two-thirds of the west wall of the Blacktail trench, and (B) the west wall of the Bear's Lair trench (Fig. 2). Trench logging at scales of 1:8 to 1:20 followed standard methods (McCalpin, 1996, p. 56–75), supplemented with 1:8-scale photomosaics of 1–4-m-wide sections of trench wall. Radiocarbon ages (triangles) are in thousands of calibrated (approximate solar) years B.P. (before A.D. 1950) rounded to the nearest century (Table DR1 [see footnote 1 in text]; complete sample location and data in Nelson et al., 2002). Unit labels next to patterns (those used by Nelson et al., 2002) and selected labels on units are those in text or shown in Figure 6. *Unit patterns do not imply correlations among trenches.* In A and B, the scarp formed through folding of all units except alluvium, colluvium, and root-stirred sediment. We infer north-dipping reverse faults beneath the folds below the floors of each trench.

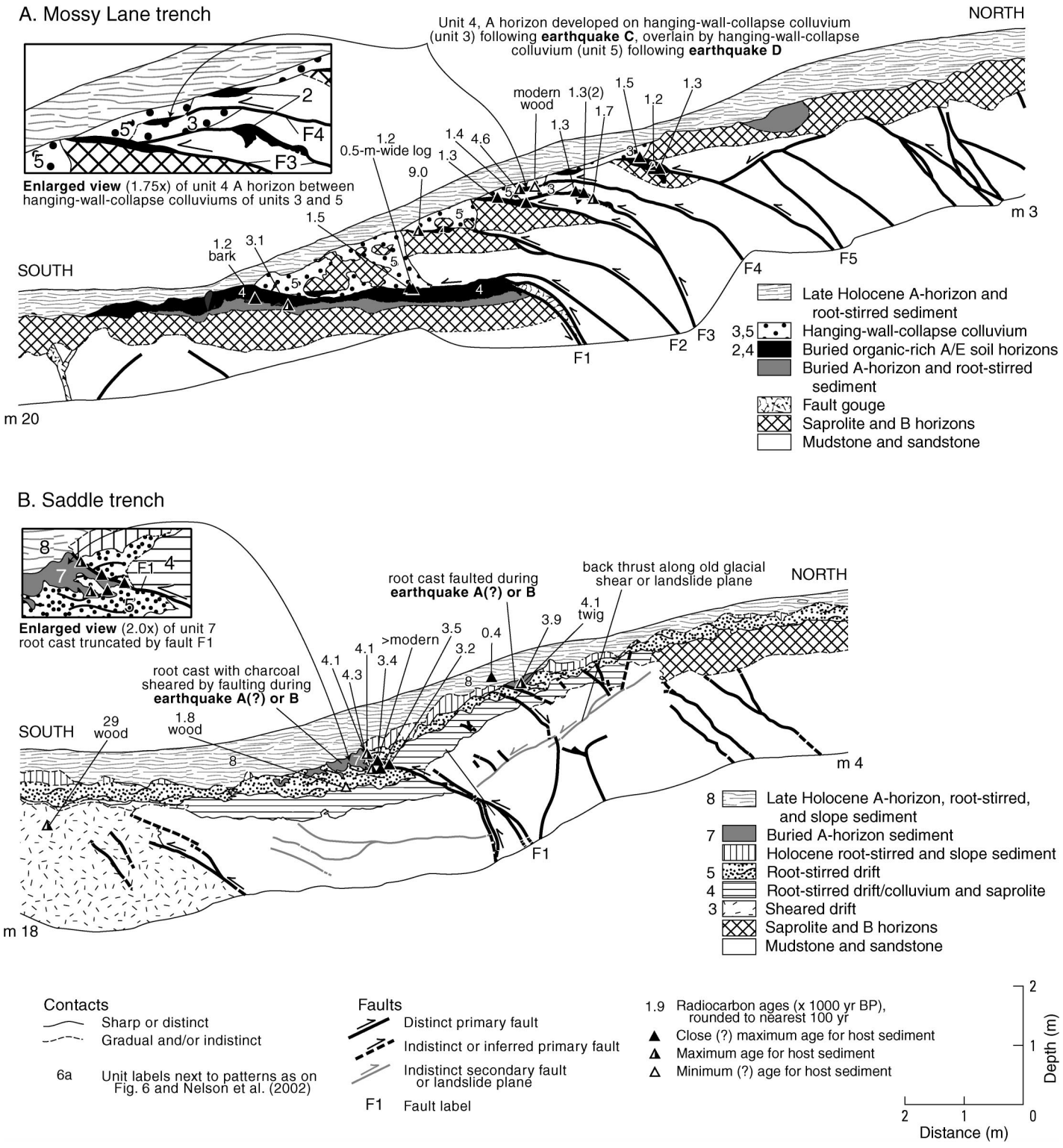

Figure 4. Simplified stratigraphy of (A) the central two-thirds of the east wall of the Mossy Lane trench, and (B) the east wall of the Saddle trench (Fig. 2; logs reversed as though viewed from behind mapped wall so that scarp has same orientation as in Fig. 3). Contacts, symbols, labels, and methods as in Figure 3. In A, bedrock was thrust upward and collapsed onto slivers of forest A horizons during two late Holocene earthquakes that are too close in age to distinguish by using ^{14}C ages. Although stratigraphy shows only that slip on fault F4 postdates slip on F3, models of basinward-stepping thrusts suggest that faults F1 and F2 postdate F3 (e.g., Kelsey et al., 1998). In B, the later of two thrust events on reverse fault F1 triggered backthrusting along an old glacial shear or landslide plane.

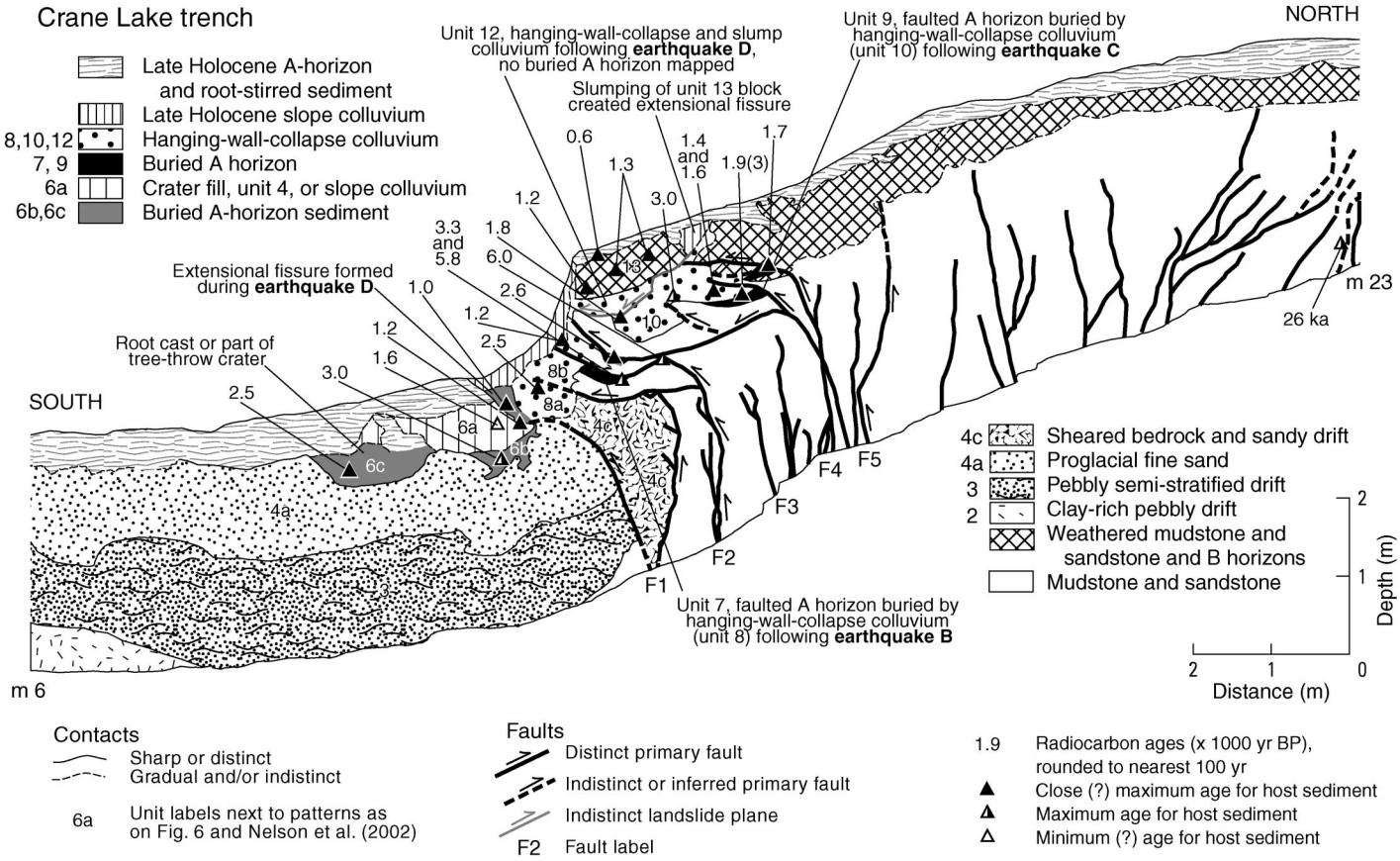

Figure 5. Simplified stratigraphy of the west wall of the Crane Lake trench (Fig. 2). Contacts, symbols, labels, and methods as in Figure 3. Faults and unit contacts between faults F1 and F5 are a composite of those mapped in two exposures <1 m apart as shown in Nelson et al. (2002). Highly weathered mudstone, sandstone, and colluvium were thrust along near-vertical faults up and over drift, younger colluvium, and A horizons during three, or possibly four, late Holocene earthquakes (Fig. 7). Charcoal dated at 26 ka in a sheared fissure in the northern part of the trench shows that some pre-Holocene faulting predates the advance of the Puget Lobe at ca. 17 ka.

landscape stability and tie stratigraphic units to scarp development.

Diatom and pollen data (Nelson et al., 2002) do not date trench stratigraphic units, but are critical in confirming the genesis and correlation of key units in the Bear's Lair and Blacktail trenches.

PRE–LATE HOLOCENE EARTHQUAKE HISTORY

Reconstruction of latest Pleistocene and Holocene landscapes at the trench sites (Fig. 6) suggests division of the earthquake history of the Toe Jam Hill fault into a Pleistocene interval before and during the last occupation of the southern lowland by the Puget Lobe glacier, ca. 17–15 ka (Porter and Swanson, 1998), and a late Holocene interval of about the past 3000 yr. We failed to find evidence of large earthquakes in any of the trenches during the intervening postglacial through middle Holocene interval.

Most evidence of Pleistocene earthquakes is fragmentary, of uncertain genesis, and undated. Mudstone and sandstone of the Miocene Blakely Harbor Formation in the Saddle, Mossy Lane, and Crane Lake trenches (Figs. 4 and 5) are pervasively faulted, folded, and fractured, and the formation's upper 0.2–1.0 m is weathered to saprolite. The geometry of many bedrock folds and faults cannot be kinematically related to the present scarp, and many structures do not extend into overlying drift, indicating that many bedrock structures predate the advance of the Puget Lobe, and perhaps the Pleistocene. In the Bear's Lair trench, footwall thickening of sandy outwash (unit 2, Fig. 3B) and the angular unconformity

Figure 6. Depositional environments and earthquake history inferred from the five trenches. Relative age is shown for environments and events prior to 16.6 ka, the time of Puget Lobe recession. Dashed gray lines outline environments that are less certain because of poorly preserved units or those of ambiguous genesis. Numbers within rectangles correspond to stratigraphic unit labels in Figs. 3, 4, 5, and 7 and those in Nelson et al. (2002). Radiocarbon triangles mark close maximum ages for environments. Inferred times of earthquakes are marked by symbols and by steps in surface offset lines. Gray symbols show uncertainty in whether or not a faulting or folding event occurred; question marks indicate uncertainty in timing that is difficult to quantify for lack of ^{14}C ages. Black vertical lines on surface offset graphs show times scarp rose; height and horizontal extent of gray lines show uncertainties in amount and timing of offsets. Uncertain origin of event A at Crane Lake is indicated by a white surface offset line.

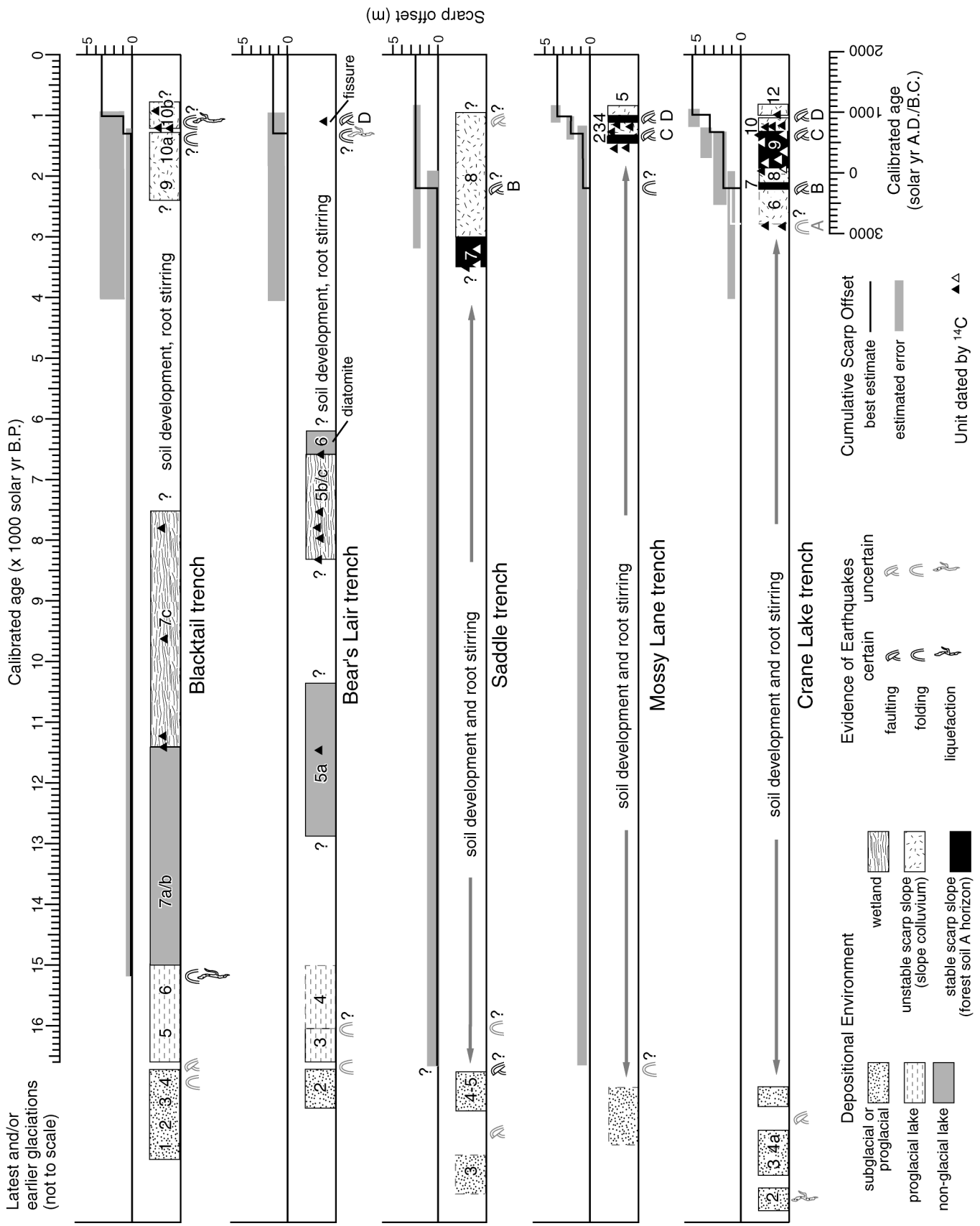
Scarp offset (m)
Calibrated age (x 1000 solar yr B.P.)
Latest and/or earlier glaciations (not to scale)
Blacktail trench
soil development, root stirring
Bear's Lair trench
diatomite
fissure
Saddle trench
soil development and root stirring
Mossy Lane trench
Crane Lake trench
Depositional Environment
subglacial or proglacial
proglacial lake
non-glacial lake
wetland
unstable scarp slope (slope colluvium)
stable scarp slope (forest soil A horizon)
Evidence of Earthquakes
certain
uncertain
faulting
folding
liquefaction
Cumulative Scarp Offset
best estimate
estimated error
Unit dated by 14C
Calibrated age (solar yr A.D./B.C.)

TABLE 1. VERTICAL COMPONENT AND RATE OF DEFORMATION INFERRED FROM TRENCHES ACROSS THE TOE JAM HILL FAULT SCARP

Surface offset and surface-deformation event(s)[†]	Total vertical displacement (m) from[‡]			Cumulative vertical displacement (m)[‡‡]	Age of datum (ka)[§§]	Vertical deformation rate (m/kyr)[##]
	Stratigraphic offset[§]	Fault slip per event[#]	Additional surface offset[††]			
Blacktail trench—3.6 m						
Post–unit 5 folding	0.2 (0.2–0.6)	–	–	3.6	15	0.24
Post–unit 8 folding	3.3 (3.1–3.5)	–	0.1	3.4	1–2.5 (<5, >0.7)	1.4–3.4
Bear's Lair trench—2.1 m						
Post–unit 3 folding	<0.2	–	–	2.1	>15	<0.14
Post–unit 5 folding	1.6 (1.5–1.6)	–	0.4 (0.4–0.6)	2.0	1–2.5 (1–5)	0.8–2.0
Fissuring event D	0.0 (–0.1–0.5)	–	–	0.0	1.0 (1.0–1.2)	0.0
Saddle trench—2.7 m						
Post–unit 4 faulting	–	0.3 (0.2–0.4)	–	2.7	>16	<0.17
Post–unit 5 folding	–	–	1.3 (0.5–1.4)	2.4	<16	>0.15
Post–unit 7 faulting event B? (and C? or D?)	1.1 (0.8–1.2)	0.5 (0.4–0.6)		1.1	2 (1–3)	0.5
Mossy Lane trench—3.5 m						
Pre-unit 3 folding	–	–	0.8 (0.4–1.3)	3.5	<16	>0.23
Faulting event C	0.8	2.0 (2.3–3.3)	–	2.7	1.2 (<1.3)	2.25
Faulting event D	1.9	8.3 (5.7–9.2)	–	1.9	1.0 (0.9–1.2)	1.90
Crane Lake trench—5.2 m			–			
Event A (?)[†††]	–	*1.1 (1.0–1.5)*[†††]	*1.0*[†††]	*5.2*[†††]	*2.5–6*	*0.87–2.08*
Faulting event B	1.0	1.9 (1.6–3.3)	–	5.2	2 (1.9–2.5)	2.36
Faulting event C	1.2	1.5 (1.5–2.1)	–	3.3	1.2 (1.2–1.7)	2.75
Faulting event D	–	1.8 (1.8–2.5)	–	1.8	1.0 (1.0–1.3)	1.80

Notes: Because fault dips in trenches range from vertical to horizontal, we tabulated only total vertical displacement (vertical component of far-field displacement across scarp from folding as well as faulting) during faulting or folding events as measured or inferred from stratigraphic relationships in trenches and surface offsets of trenched scarps. Range of uncertainty in listed values in parentheses. Dash indicates no data.

[†]Events listed from oldest to youngest. Most folding cannot be assigned to a single earthquake (Fig. 6), but stratigraphy and ^{14}C ages constrain at least the maximum age of folding. Distances following trench name are total vertical displacement (surface offset at trench site), as measured from scarp-perpendicular profiles (Nelson et al., 2002). At Bear's Lair site, where trench did not extend across entire scarp, we infer that stratigraphic (1.6 m) and surface (2.1 m) offset would agree if trench had been longer.

[‡]Vertical component of far-field displacement from faulting and folding projected into vertical plane of trench wall. Trenches are perpendicular to scarp.

[§]Vertical displacement estimated from offset of (1) same contact on either side of a structure, or (2) vertical separation of tops of buried A horizons below postfaulting ground surface (generally a minimum estimate of fault slip because of difficulty of determining position of former ground surfaces).

[#]Vertical slip estimated by summing slip measured from piercing points along one or more faults; uncertainties in piercing points, in presence of inferred faults, and in whether slip occurred on a particular fault during a particular earthquake give large ranges in slip values. Values are commonly maximums because of hanging-wall distention.

[††]Remainder of total vertical displacement indicated by surface offset across scarp (column 1) that is unaccounted for in columns 2 and 3. Stratigraphy and trench correlation suggest that all or most additional displacement occurred through folding during middle or late Holocene, but recession of Puget Lobe at ca. 16–15 ka is the only certain prefolding datum at upland sites.

[‡‡]Cumulative total vertical displacement using our preferred estimates (columns 2–4, those values not in parentheses). Preferred estimates are based on sequence of deformation events in a trench, total surface offset, and correlation of deformation events among trenches (Fig. 6).

[§§]Estimated (ka, thousand years B.P.) from ages in Figures 3–5 and in Table DR1 (see text footnote 1) as explained in text; ages shown to one decimal point are based on ^{14}C ages in calibrated (approximate solar) years B.P. (before present [A.D. 1950]) rounded to nearest century. Complete stratigraphic and ^{14}C data in Nelson et al. (2002).

[##]Rate calculated from cumulative total vertical displacement (column 5) divided by time from datum (column 6) to present (k.y., time interval in thousands of years).

[†††]As explained in text, the evidence for event A may or may not record an earthquake. Values shown in italics assume that event A records a surface-faulting or -folding earthquake. Values for faulting event B assume that event A is nontectonic and that all pre–event C displacement occurred during earthquake B.

between the outwash and overlying proglacial lake deposits (unit 3) might record an earthquake. A thicker sequence of drift and outwash beneath the same unconformity in the Blacktail trench (unit 3/unit 5 contact, Fig. 3A) is extensively deformed, probably through the collapse of stagnant ice and glacier movement. Some of this deformation, such as a small low-angle (if we restore later tilting) normal fault, may be tectonic. Even if coseismic, the estimated vertical offset across these possible late Pleistocene faults and folds is small (<0.5 m, probably ~0.2 m).

Laminated proglacial lake sediment in the Blacktail (units 5 and 6, Fig. 3A) and Bear's Lair (units 3 and 4, Fig. 3B) trenches, probably deposited during the recession of the Puget Lobe at ca. 16–15 ka (Porter and Swanson, 1998), shows signs of at least one earthquake. Fine sand liquefaction dikes in the Blacktail lake beds derived from underlying sandy outwash are distinct from dikes intruding younger Holocene lake mud. The combination of dikes and fluid-escape structures in the lake beds that do not extend into Holocene sediment (unit 7) and decreasing dips up-section in the beds and underlying units suggests earthquake-related folding, most likely soon after deposition. Total vertical displacement (vertical component of far-field displacement across scarp from folding and faulting) at the Blacktail site during folding was 0.2–0.6 m on the basis of the dip change of 2°–10° and assuming a 6 m limb width (Table 1). In the Bear's Lair trench, slight folding (<0.2 m total vertical displacement) of lake beds (unit 3) with distinct fluid-escape structures might also be coseismic.

Nonglacial lake and wetland sediment in the Blacktail and Bear's Lair trenches, probably spanning much of the 15–6 ka interval, rules out large surface-deformation events along the scarp during much of postglacial through middle Holocene time. More clay-rich texture than in underlying proglacial lake beds, massive structure due to bioturbation, greenish-brown color (2Y hue) reflecting finely disseminated organic material, and poorly preserved diatom assemblages representative of small lakes or ponds show that the lake mud was deposited during a climate similar to that of the present. The lack of any weathering horizons between proglacial lake beds and overlying lake mud suggests one or more temperate lakes formed early in the postglacial period. Radiocarbon ages show that the lake(s) had gradually shoaled into wetland(s) by ca. 11.4 ka at the Blacktail site and by 8.3 ka at the Bear's Lair site (Fig. 6; Table DR1 [see footnote 1]). Ages in, or just above, wetland peat show that wetlands persisted until at least 7.5 ka and perhaps to ca. 6 ka. Pods of root-stirred white diatomite above wetland peat in

the Bear's Lair trench record the brief return of a middle Holocene lake in which diatoms flourished.

By using stratigraphy and soils in the Blacktail and Bear's Lair trenches, we infer that the absence of earthquakes extended to the late Holocene (Fig. 6). Moderate to strong prismatic ped structure in argillic B horizons developed on Holocene lake mud (Nelson et al., 2002) indicate thousands of years between the end of wetland deposition and late Holocene folding (discussed subsequently) at the two wetland sites. Remnants of clay-rich argillic horizons are also widely preserved on old drift and weathered bedrock in the three upland trenches, but pronounced root stirring of the upper 0.3–0.5 m of scarp sediment limits our confidence in using stratigraphy to infer an absence of earthquakes from postglacial through middle Holocene time at the upland sites. If pre–late Holocene earthquakes as large as those of the late Holocene had ruptured the ground surface at any of the five trench sites, we would expect at least one of the five trenches to have exposed remnants of pre–late Holocene A horizons under fault hanging walls and/or thick deposits of hanging-wall-collapse colluvium. No such evidence was found.

A CLUSTER OF LATE HOLOCENE EARTHQUAKES

We reconstruct a history of three, and possibly four, late Holocene earthquakes on the Toe Jam Hill scarp from a synthesis of stratigraphy and structure in the five trenches. Monoclinal folds in the Blacktail and Bear's Lair trenches could have formed in a single earthquake, but more extensively dated thrusting in the Crane Lake and Mossy Lane trenches records three earthquakes in the short interval 2.5 ka to 1.0 ka. From this we infer the scarps underlain by folds to be the product of progressive folding during multiple earthquakes. Complex patterns of surface rupture may have led to one or two of the earthquakes producing minimal surface deformation (<0.5 m vertical offset) at some sites. Maximum-limiting ^{14}C ages on detrital charcoal in faulted deposits cannot be used to distinguish earthquakes in such a short interval of time. The ages do, however, provide age constraints that help in correlating earthquakes, especially between the Crane Lake and Mossy Lane sites. We group evidence for earthquakes in the other trenches with the most likely correlative earthquake(s) at Crane Lake and Mossy Lane (Fig. 6).

Event A

The possibility of an earliest late Holocene earthquake (event A, Figs. 6 and 7) depends on the interpretation of unit 6a in the Crane Lake trench. A nontectonic interpretation of event A is that unit 6a consists of sediment eroded from large pieces of proglacial sand (unit 4a) raised in the root ball of a toppled tree; unit 6a now fills the tree's former crater (panel 1, Fig. 7). In this interpretation, units 6b and 6c are casts of the tree's roots, or perhaps the lowest part of the crater, now filled with organic-rich A-horizon sediment. Such inverted soil stratigraphy is typical of fills in tree-throw craters. Unit 4a, the only unit with a lithology similar to that of unit 6a, is the only possible source for 6a. Examination of units 4a and 6a at 6–25× magnification shows that the only lithologic difference between them is that 6a contains more silt than unit 4a with a few rounded pebbles and is very weakly cemented. A problem with the tree-throw interpretation is that we found no signs of roots or wood fragments in unit 6a. If unit 6a is tree-throw fill, a ^{14}C age from unit 6c suggests that the tree fell after 2.5 ka (Fig. 5; Table DR1 [see footnote 1]). The only age from unit 6a (1.6 ka) is so young that we infer that it was measured on charcoal introduced into the unit along a later root channel or fracture.

Alternatively, unit 6a formed in response to the first of four late Holocene earthquakes, either as (1) the upper part of unit 4a that was folded into a low scarp (folding hypothesis), or (2) a distal wedge of scarp-derived slope colluvium eroded from a collapsed hanging wall (faulting hypothesis). Folding implies units 6b and 6c to be root casts unrelated to tree throw, but does not adequately explain their present depth and preservation at the base of the scarp. If the folding hypothesis is correct and the casts formed after folding, then folding may predate charcoal in the casts dated at 2.5–3.0 ka (Fig. 5). Chief problems with the surface-faulting hypothesis are that no forest soil is buried by the hypothesized wedge of scarp colluvium (panel 1, Fig. 7), the wedge contains no clasts eroded from weathered bedrock that would have been exposed in the hanging wall of the fault, and similar wedges of distal slope colluvium produced during younger faulting events were not identified. If the faulting hypothesis is correct, the root casts and the charcoal in them (2.5–3.0 ka) predate faulting. On the basis of stratigraphic offset estimates for later earthquakes and surface offset across the scarp, stratigraphic offset during the possible earthquake of event A—whether due to folding or faulting—would have been about 1 m (Table 1).

Too little evidence is preserved to rule out tectonic or nontectonic hypotheses for event A. All hypotheses suffer from the absence of unit 4a or any other sandy units in the present hanging wall of the Crane Lake trench that could be a potential source for unit 6a (Fig. 5). Maximum ages for faulting in the Saddle trench, correlated in the following section with earthquake B (Fig. 6), permit correlation of the Saddle faulting with event A at Crane Lake. And part of the undated folding and liquefaction recorded in the Blacktail, Bear's Lair, and Mossy Lane trenches could conceivably have occurred during event A. Because we are uncertain of the origin and age of event A, we do not consider it in estimating earthquake recurrence.

Earthquake B

Surface faulting during earthquake B is recorded best by an A horizon (unit 7) buried by fault-generated colluvium (unit 8) in the Crane Lake trench (Figs. 5, 6, and 7). From the heterogeneity of unit 8's diamicton lithology, particularly its small deformed lenses of organic-rich sediment (derived from unit 7), we infer that unit 8 is hanging-wall-collapse colluvium derived from root-stirred unit 4a, weathered bedrock, and remnants of thin sandy drift exposed at the far north end of the trench (complete trench log in Nelson et al., 2002). Thrusting along faults F1–F4 raised tongues of bedrock and unit 4a, which then collapsed to form units 8a and 8b/8c and bury slivers of the A horizon (unit 7) developed on bedrock (panel 2, Fig. 7). During earthquake B (and probably earlier surface-faulting earthquakes), shearing, shortening, and thickening of pebbly drift (unit 3), unit 4a, and bedrock between faults F1 and F3 produced highly deformed unit 4c (Fig. 5).

Reconstruction of the slivers of the A horizon of unit 7 suggests ~0.6–1.2 m of slip on faults F1–F3 during earthquake B. Slip on F4 could have been as much as 1.2 m if event A failed to produce a scarp, but some of the slip can also be assigned to later faulting events. On the basis of reconstructed fault slip and the 5.2 m of surface offset across the scarp, we estimate ~1.9 m of vertical slip for earthquake B if event A is nontectonic and ~0.9 m if event A resulted in a scarp (Table 1).

Earthquake B is younger than the youngest ^{14}C ages from units 7 and 8 (2.5 and 2.6 ka) and older than the oldest ages of 1.9 ka on unreworked charcoal from a younger A hori-

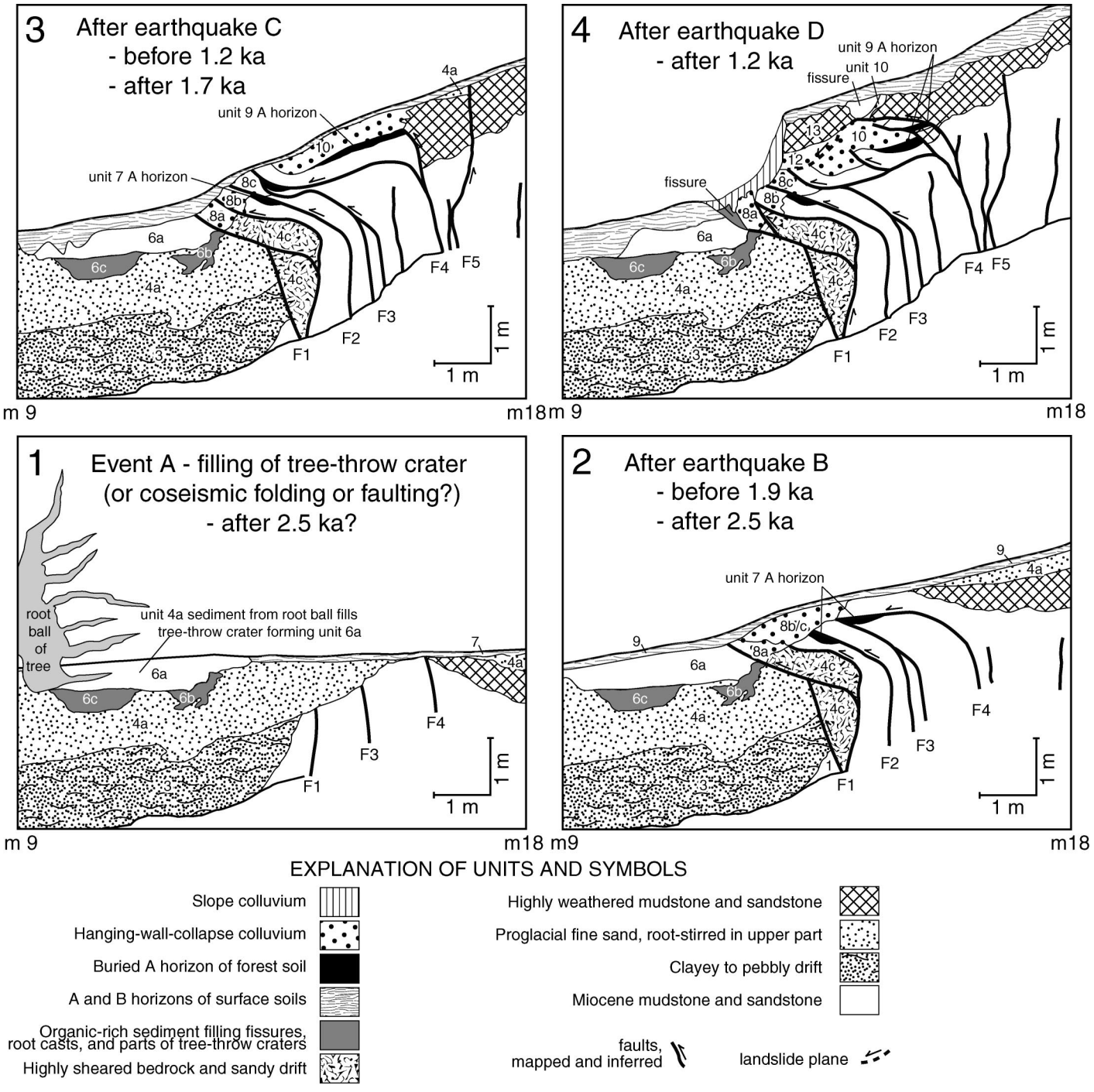

Figure 7. Reconstruction of sequence of surface-deforming earthquakes at Crane Lake inferred by retrodeforming the stratigraphic units. Selected units are labeled as in Figures 5 and 6. Time constraints based on ^{14}C ages in Figure 5 and Table DR1 (see footnote 1 in text). Panel 1 shows how unit 6a may have formed through filling of a tree-throw crater. Alternatively, 6a might have been deposited as a scarp-derived colluvial wedge following folding or faulting of Miocene bedrock, pebbly drift, and proglacial sand (unit 4a) prior to earthquake B. During earthquake B (panel 2), bedrock and proglacial sand were thrust upward and over drift, sand, and root casts and a tree-throw crater, slivering the A horizon of a forest soil (unit 7). The hanging wall then collapsed, burying the soil with the first hanging-wall-collapse colluvium (unit 8). During earthquake C (panel 3), most slip probably occurred on faults F2–F4, truncating the A horizon of a new forest soil developing on the scarp (unit 9), burying the soil with a second hanging-wall-collapse colluvium (unit 10) consisting of bedrock and root-stirred remnants of proglacial sand, faulting the first hanging-wall-collapse colluvium (unit 8), and thrusting a tongue of bedrock over the top of it. Slip on fault F4 during earthquake D (panel 4) slivered the A horizon (unit 9), faulted the second collapse colluvium (unit 10), and thrust a block of weathered bedrock (unit 13) out over it. The block then slumped, producing the third collapse colluvium (unit 12) and a head-scarp fissure.

zon (unit 9; Fig. 5; Table DR1 [see footnote 1]). Because unit 8b is so deformed, its 2.5 ka charcoal might have been introduced into the unit along an unrecognized root channel or fracture and so provide a minimum age for earthquake B. But such an explanation is unlikely for the 2.6 ka age from the clay-rich sliver of unit 7, encased in sticky saprolitic mudstone. The minimum interval separating event A from earthquake B is the amount of time required for the A horizon of unit 7 to form (probably decades).

We also found evidence of surface faulting probably correlative with earthquake B in the Saddle trench where charcoal dated at 3.2–4.3 ka in faulted root casts (eight ages near fault F1 in Fig. 4B, enlarged view; Table DR1 [see footnote 1]) shows thrusting on fault F1 and a secondary backthrust to be younger than the youngest dated charcoal (3.2 ka). Although the ages permit correlation of the thrusting with any of the late Holocene earthquakes (A–D), we favor a correlation with earthquake B because a tectonic origin for event A is uncertain and the ages are older than most of those associated with earthquakes C and D in other trenches. As in the Crane Lake trench, the root casts of the Saddle trench are distinct from other units because they (1) are young enough (late Holocene) to retain dark-colored organic material from the A-horizon sediment that fills them, and (2) have been protected from later root stirring by partial overriding by the hanging wall, collapse of the thrust tip, and rapid deposition of slope colluvium deposited in response to faulting. In the Saddle trench, slip along fault F1 (as measured from unit 5 contacts, Fig. 4B) about the time of earthquake B was ~0.5 m but would increase to 1.1 m if tectonic folding within several meters of the fault is included (Table 1).

Lack of ^{14}C ages hampers our apportionment of the folding in the Mossy Lane, Bear's Lair, and Blacktail trenches among earthquakes B, C, and possible earthquake A (Fig. 6). In the Mossy Lane trench, folding is required to account for the difference (0.8 m) between the present surface offset (3.5 m) and the vertical slip that occurred during the two latest Holocene earthquakes (Table 1). Part of the 3.3 m of postwetland (i.e., younger than 7.6 ka) stratigraphic offset in the Blacktail trench might have occurred during earthquake B, although from ^{14}C ages in colluvium overlying the fold (discussed later) we infer that most offset occurred later in the Holocene (Fig. 6). In the Bear's Lair trench, ~1.6 m of stratigraphic offset, caused by folding and accompanied by minor dewatering or liquefaction, postdates wetland deposits dated at 7.5 ka and so could be assigned to the middle or late Holocene. In both wetland trenches, the postwetland development of argillic soil horizons on lake sediment indicates at least several thousand of years of soil development, supporting middle Holocene slope stability followed by late Holocene folding.

Earthquake C

The chief evidence for earthquake C is hanging-wall-collapse colluvium thrust over A horizons in the Crane Lake and Mossy Lane trenches (Figs. 4A and 5). At Crane Lake, additional slip on faults F1–F4 of perhaps 0.7–1.3 m (estimated from cumulative offsets of unit contacts, Table 1 notes; panel 3, Fig. 7) displaced the hanging-wall-collapse colluvium produced during earthquake B (unit 8). Thrusting of weathered bedrock and root-stirred remnants of unit 4a along the higher splay of fault F4 resulted in offset of at least 0.8 m and truncated the A horizon of unit 9. The subsequent collapse of the hanging wall onto unit 9 produced a sandy colluvium (unit 10) lithologically similar to unit 8b. At the same time, a tongue of weathered bedrock rode up over the top of unit 8c to buttress the tip of unit 10.

Consistent ages on detrital charcoal in the Crane Lake trench suggest an age of ca. 1.7 to 1.2 ka for earthquake C. Pieces of branch or trunk charcoal several centimeters long in two exposures of the unit 9 A horizon are well dated at 1.7–1.9 ka, and small fragments of charcoal within unit 10 give ages as young as 1.4 ka (Fig. 5; Table DR1 [see footnote 1]). Overlying colluvium from the most recent earthquake (D; unit 12) yields ages of 1.3–1.2 ka.

In the Mossy Lane trench near the tip of fault F4, an A horizon (unit 4) developed on hanging-wall-collapse colluvium (unit 3) is buried by later hanging-wall-collapse colluvium (unit 5), showing that the young reverse faults in this trench (F1–F5) slipped during at least two earthquakes (Fig. 4A, enlarged view). Twelve ^{14}C ages on slivers of soil buried during the earthquakes range from 1.7 to 1.2 ka; and ages as young as 1.2 ka come from soil slivers buried during each earthquake (Table DR1 [see footnote 1]). These data imply an interval between earthquakes shorter than the 200- to 300-yr uncertainties on the charcoal ages. Although the Mossy Lane ages fall at the younger limit of our age range for earthquake C in the Crane Lake trench, we correlate the first earthquake in the Mossy Lane trench with earthquake C in the Crane Lake trench (Fig. 6), which implies an age for earthquake C of ca. 1.3–1.2 ka. Not making this correlation requires the two latest faulting events in both trenches to be the result of three earthquakes.

Could our evidence for earthquakes B and C in the Crane Lake trench have been produced by a single earthquake at ca. 1.3–1.2 ka? Lithologic, stratigraphic, and structural evidence make this alternative unlikely (Figs. 5 and 7): (1) the sandy, more homogeneous lithology of unit 10 relative to unit 8 suggests that the units were derived from different sources in the hanging wall at different times, (2) unit 8 was more severely deformed than unit 10, probably during multiple faulting events, and (3) a single earthquake would require the lower contact of unit 10 to be a fault and close scrutiny of this contact showed no evidence of slip.

No evidence of earthquakes correlative with earthquake C was identified in the Blacktail, Bear's Lair, and Saddle trenches. On the basis of our estimates of total vertical displacement at Crane Lake and Mossy Lane (Table 1), the largest proportion of displacement at these other sites likely occurred during earthquake D rather than earthquake C.

Earthquake D

The most recent earthquake (D) was probably the largest; evidence for it is widespread and distinct in at least three trenches (Fig. 6). In the Crane Lake trench, slip along several splays of fault F4 slivered the A horizon of unit 9, overthickened the collapse colluvium of unit 10, and thrust a block of weathered bedrock (unit 13) over unit 10 (Figs. 5 and 7). Sliver realignment suggests 1.0–1.2 m of slip on F4 faults, and less slip (probably $<$0.4 m) may have occurred on faults F1–F3. As the block of unit 13 was thrust southward over unit 10, its lower part fractured and disaggregated into collapse colluvium (unit 12), allowing the block to break away from the hanging wall (forming a fissure, Fig. 5), tilt, and then slide ~0.8 m down slope. Some movement was by fragmentation of the lower part of the block and fragment rotation. Buttressing by the underlying tongue of bedrock prevented the block from sliding, rotating, and disaggregating completely to build a wedge of colluvium near the base of the scarp. Subtracting our estimate of (nontectonic) distension through fragmentation in the 1-m-long hanging-wall block yields slip on F4 faults of ~1.8–2.0 m for earthquake D, and total slip for earthquake D on faults F1–F4 of ~1.8–2.5 m (Table 1). A thin slope colluvium containing many fragments derived from the unit 13

block drapes the lower scarp slope and partly fills an extensional fissure that opened at the base of the scarp (Fig. 5). Such fissures are common on the scarps of historic reverse-fault ruptures (Philip et al., 1992; Bilham and Yu, 2000; Kelson et al., 2001).

The absence of a mapped A horizon on unit 10 colluvium in the Crane Lake trench raises the question of whether the evidence attributed to earthquakes C and D in this trench could have formed during the same earthquake. A horizons buried by collapsed hanging walls are the strongest evidence of earthquakes B and C at Crane Lake and earthquakes C and D at Mossy Lane (Figs. 5 and 4A). Because we consider it unlikely that unit 10 colluvium was simultaneously deposited on unit 9, faulted, and overridden by the unit 13 block, we favor a two-earthquake interpretation (panels 3 and 4, Fig. 7). Units 10 and 12 differ more in lithology and degree of consolidation than other colluvial deposits in the trench, and the planar contact between them suggests slumping or sliding of units 12 and 13 over unit 10 long after it was deposited rather than deposition of all units within the same collapsed hanging wall. Fragments of organic-rich sediment in unit 12 may be remnants of an unrecognized A horizon on unit 10 disturbed by overriding units.

During earthquake D at Mossy Lane, simultaneous slip on faults F1–F4 thrust bedrock, saprolite, and forest soil over bedrock, saprolite, hanging-wall-collapse colluvium from earthquake C (unit 3), and the woody A horizon and underlying sandy E horizon that mantled the scarp prior to faulting (unit 4). Bedrock, colluvium, and soil were thrust upward and then collapsed southward onto the scarp (Fig. 4A). Large and small blocks of saprolite near the tip of fault F1, including one as shown by its A horizon to have rotated upside down, stand out in the thick wedge of collapse colluvium that buries the thick, woody soil of unit 4. Near the tip of fault F3, a sandwiched A horizon (unit 4) developed on unit 3 shows that during earthquake D, a hanging-wall-collapse colluvium (unit 5) buried the almost identical collapse colluvium from earthquake C (unit 3; enlarged view in Fig. 4A). Net slips for earthquake D along the four faults (total slip of 8.3 m) are F1—2.7 m, F2—1.7 m, F3—2.7 m, and F4—1.2 m. Because the faults have such shallow dips, the vertical component of slip for earthquake D is only 1.9 m (Table 1).

In the Bear's Lair trench, a rust-stained, graben-like fissure with minimal net offset is the only evidence we confidently correlate with earthquake D (Fig. 3B). Radiocarbon ages on wood and charcoal within small blocks of peaty mud caught in the middle of the 1-m-wide, 3-m-deep fissure show that it formed after 1.5 ka (Table DR1 [see footnote 1]). Because of insufficient identifiable stratigraphic units and few ^{14}C ages in the Bear's Lair trench, we are unable to determine how much, if any, of the 1.6 m of middle and late Holocene stratigraphic offset caused by folding coincided with earthquake D.

Close agreement among ^{14}C ages on large or delicate samples from units displaced by, or produced in response to, faulting support correlation of the most recent deformation features in the Mossy Lane and Bear's Lair trenches with earthquake D in the Crane Lake trench and with the 1050–1020 cal. yr B.P. earthquake that produced terrace uplift and a tsunami in Puget Sound. Ages from the colluvium of unit 12 at Crane Lake, deposited following earthquake D, indicate that it formed after 1.2–1.3 ka (Fig. 5; Table DR1 [see footnote 1]). The fissure at the base of the Crane Lake scarp contains the largest, least decayed pieces of charcoal in the trench, dated at 1.2–1.0 ka (youngest age, 1060–920 cal. yr B.P.). The age on a western red cedar leaf attached to a 2-cm-long block of peaty mud at the base of the fissure in the Bear's Lair trench dates the fissure's opening to shortly after 1.1 ka (1230–960 cal. yr B.P.). The little-decayed leaf is part of the loose forest floor litter that fell into the fissure. The most precise age for earthquake D (1300 $\pm$ 21 ^{14}C yr B.P., 1290–1170 cal. yr B.P.) comes from averaging four ages on the outer 7–10 rings of a $>$0.5-m-wide burned log squashed on the forest floor at Mossy Lane by the collapse of the fault F1 hanging wall (Fig. 4A). If our correlation of earthquake D with the 1050–1020 cal. yr B.P. earthquake is correct, the log was $>$120 yr old at the time of the earthquake.

At least the most recent rise of the Blacktail scarp coincides with earthquake D (Fig. 6). Three ages of 1.2 ka or younger from two thin wedges of slope colluvium on the Blacktail scarp (units 10a and 10b, Fig. 3A; Table DR1 [see footnote 1]) suggest scarp instability, probably due to folding, about this time. Although the ages are too few to determine whether units 10a and 10b differ in age, linear reddish-orange zones near the tops of the units—probably A- and B-horizon sediment baked by fires—suggest horizons that mark times of relative slope stability following the deposition of each colluvial unit. In Figure 6 we assume two periods of colluvial deposition due to late Holocene folding and apportion the 3.4 m of total vertical displacement measured in the Blacktail trench between two folding events. On the basis of inferred relative proportions of total vertical displacement for earthquakes C and D in the Crane Lake and Mossy Lane trenches (Table 1), we hypothesize that vertical displacement during the youngest folding event at Blacktail was greater than that during the earlier earthquake(s).

Hand-core data from the wetland adjacent to the Blacktail scarp lend support to the hypothesis that most deformation of the Blacktail scarp occurred during one large folding event or several events closely spaced in time. About 4 m of *Typha* and *Sphagnum* peat, which overlies silty lake sediment containing the 6.8 ka Mazama ash (Zdanowicz et al., 1999; A. Sarna-Wojcicki, 2000, written commun.), thins to 1–2 m of peat and muddy peat near the scarp. Cores $\sim$4 m from the scarp show only one thin lens of sandy pebbly muddy peat at a depth of 0.25–0.35 m, whereas cores farther from the scarp lack sandy pebbly lenses that might record pulses of sediment eroded from the scarp following an earthquake. In contrast, cores 2 m from the scarp show muddy peat with much sand and pebbles, but lack distinct sandy lenses separated by peat that would reflect alternating episodes of scarp erosion and stability caused by earthquakes recurring many hundreds of years apart.

Extensive liquefaction deposits (unit 8), exposed in the Blacktail trench, were formed during earthquakes C or D. Liquefaction features intrude all the folded post–Puget Lobe units in the trench and are tilted parallel with them (Fig. 3A). The features may have been intruded during earthquake C and tilted during folding of the intruded beds during earthquake D. Alternatively, liquefaction might have occurred during earthquake D only moments before the folding.

We found no direct evidence in the Saddle trench for earthquakes C or D, although at least some of the folding with a 1.1 m vertical component discussed under earthquake B may well have occurred during the younger earthquakes. The unusually thick blanket of organic-rich slope colluvium (unit 8, Fig. 4B) at the base of the Saddle scarp may partly reflect latest Holocene deformation. The 1.8 ka age from a decayed root in a partly filled root cast is clearly younger than the overlying faulted root casts, and the root is unusually deep for its age. Because the ground surface was probably at least 0.5 m closer to the cast when its root was growing, we infer the lower scarp to be buried by at least 0.5 m of slope colluvium. Perhaps rapid deposition of the colluvium was a response to folding or faulting during the most recent earthquake(s).

EARTHQUAKE HAZARD

Fault Slip per Earthquake and Postglacial Vertical Deformation Rate

The amount of fault slip at the surface along the Toe Jam Hill fault during each late Holocene earthquake is difficult to estimate; some faults never reach the surface (Fig. 3), others change dip as much as 90° within a few meters of the surface (Figs. 4 and 5), and the complex collapsed-hanging-wall stratigraphy of some faults yields few precise measurements. For this reason, we estimate the vertical component of far-field displacement across the scarp (total vertical displacement) for each folding or faulting event by summing stratigraphic offsets across structures, vertical separations of buried A horizons, and slip along faults that show stratigraphic offsets that date to about the same time (Table 1). Differences between summed vertical slip and vertical surface offset are attributed to folding. Folding may have preceded surface faulting by hundreds to thousands of years, or folding may have coincided with faulting.

Total vertical displacement during even the most certain of the probable pre-Holocene earthquakes was <1.3 m (Table 1; Fig. 3), probably <0.3 m if our reconstruction of scarp development in the Blacktail, Saddle, and Mossy Lane trenches is correct (Fig. 6). Thus, the Toe Jam Hill fault history offers little support for the burst of faulting during deglaciation hypothesized for the Seattle fault zone by Thorson (1996, 2000b).

Slip rates for the Toe Jam Hill fault are difficult to evaluate in comparison with rates for the Seattle fault zone for two reasons. (1) Toe Jam Hill fault-slip rates vary by a factor of at least four depending on the interval of time considered: postglacial (after 16 ka) rates are 0.2–0.3 mm/yr, whereas post–3 ka rates are 0.8–3.4 mm/yr (Table 1). (2) The proportion of north-south shortening contributed by slip on the Toe Jam Hill fault during earthquakes on the Seattle fault and other faults in the Seattle fault zone is unknown and may have changed over time. Johnson et al. (1999) suggested a postglacial dip-slip rate of 0.7–1.1 mm/yr for the entire Seattle fault zone, consistent with recent estimates by Calvert et al. (2001) and with Thorson's (1996) glacial stratigraphy estimate of 8–14 m of postglacial offset across the zone at Alki Point (Fig. 1). The factor of three lower postglacial dip-slip rates for the Toe Jam Hill fault suggests that about a third of postglacial slip in the zone is taken up by the Toe Jam Hill fault, but the Seattle fault's lack of prominent scarps along its surface projection complicates this inference. Perhaps near-surface slip on the Seattle fault is widely distributed on many small faults or expressed as broad folding. Alternatively, much slip on the Seattle fault at depth may have propagated to the surface along the Toe Jam Hill fault rather than largely on the Seattle fault (Fig. 1C), at least during some earthquakes. For example, main thrust to backthrust relationships during the 1999 Chi-Chi earthquake in Taiwan indicate 30%–40% of the main thrust slip occurred on a backthrust, and uplifted terraces suggest a similar distribution of cumulative slip from past earthquakes (Ota et al., 2003). In comparison with the postglacial slip rate for the Seattle fault zone, the high rates of late Holocene slip for the Toe Jam Hill fault probably reflect an unusual cluster of earthquakes on one fault strand along one part of the fault zone rather than a recent increase in the rate of north-south shortening across the entire fault zone.

Recurrence

Postglacial (since 16 ka) recurrence intervals for earthquakes recorded in the Toe Jam Hill fault trenches range from ~0.2 to 12 k.y. The longest apparent interval, from the most recent of the postglacial earthquakes to earthquake B, is probably 10–12 k.y. (Fig. 6). The wide distribution of Holocene lake sediment in the wetland trenches and the absence of pre–late Holocene collapse colluvium in their upland counterparts allow us to preclude surface-deforming earthquakes for much of the 10-to-12-k.y.-long interval. Late Holocene history is different, with a cluster of three, or possibly four earthquakes closely spaced in time.

Radiocarbon ages constrain the interval between earthquakes C and D in the Crane Lake and Mossy Lane trenches to less than ~250 yr, and A horizons separated by hanging-wall-collapse colluvium indicate at least decades between the earthquakes. Earthquake B occurred between 2.5 and 1.9 ka, and the dark color (high organic content) of the A horizon of unit 7 in the Crane Lake trench suggests at least decades of soil development between it and earthquake C. Radiocarbon constraints on the times of earthquakes B and C combined with the range of estimates for the intervals between earthquakes C and D indicate that the interval between B and C could be as great as 1300 yr or as little as 200 yr (Fig. 7). The interval between event (possible earthquake) A and earthquake B may range from a few hundred to a few thousand years depending on whether late Holocene root casts at the toe of the scarp pre- or postdate event A.

If, as we infer, the Toe Jam Hill fault is a backthrust that is slip dependent on its master fault, the Seattle fault, the history of the Toe Jam Hill fault is at least a partial proxy for the history of the Seattle fault. From a detailed paleoecologic reconstruction of marsh history at Restoration Point, 1.6 km southeast of the Toe Jam Hill fault (Fig. 2), Sherrod et al. (2000) identified only one large earthquake on the Seattle fault since 7 ka, the 1050–1020 cal. yr B.P. earthquake. Although Sherrod et al. (2000) attributed the down-core variation in their paleoecologic parameters to beach bar movement at the gateway to the marsh, they left room in their reconstruction for possible land-level changes during earthquakes at ca. 7.2–6.4 ka, 3.5–2.0 ka, and 1.9–1.5 ka. The younger two intervals coincide with our estimates for the times of event A and earthquake B.

Although we correlate earthquake D on the Toe Jam Hill fault with the 1050–1020 cal. yr B.P. earthquake on the Seattle fault, the emerging tally of prehistoric earthquakes in the southern Puget Lowland includes earthquakes that may pre- or postdate the 1050–1020 cal. yr B.P. earthquake. In addition to tsunami-laid sand and liquefaction dikes dated to about the time of that earthquake, Bourgeois and Johnson (2001) described younger liquefaction features and possible subsidence stratigraphy, as well as older sand laminae of possible tsunami origin, from intertidal outcrops spanning ~1900 yr in the Snohomish River delta near Everett (Fig. 1A). Sherrod (2001) suggested that the large subsidence at two intertidal sites might be explained by two earthquakes closely spaced in time, one of which might correlate with a post–1020 cal. yr B.P. earthquake recorded at the Snohomish River. In the Seattle fault zone, Harding et al.'s (2002) analysis of shoreline heights measured from ALSM imagery along transects that intersect projections of backthrusts near Alki Point and Bainbridge Island (Fig. 1B) shows steps that may record small offsets along these faults and other unmapped faults in the zone. The undated scarps might record multiple earthquakes in the Seattle fault zone. Near the eastern end of the Seattle fault in Lake Washington, Karlin and Abella (1996) proposed that at least the most distinctive of 41 silty lake beds deposited since 12 ka are earthquake-induced turbidites. Thorson (2000a), who attributed many silty lake beds in Lake Washington to nonseismic shoreline erosion, inferred that some of 21 abrupt lithologic contacts in peaty shallow-water lake sediment deposited between 6 ka and 1 ka re-

cord submergence during earthquakes on the Seattle fault zone. Most recently, multiple surface ruptures at four sites on the Seattle fault 12–16 km east of Seattle likely predate the late Holocene (Sherrod, 2002).

Rupture Extent

Evaluation of the length of the Toe Jam Hill fault rupture during late Holocene earthquakes is limited to the 2.6 km width of southern Bainbridge Island (Fig. 2), although late Holocene rupture on an en echelon scarp near Waterman Point, 3 km to the southwest, may extend the limits of surface rupture to 5 km (Haugerud et al., 2003). Because the Toe Jam Hill fault scarp does not perturb the island's lowest east-coast marine terrace, Bucknam et al. (1999) and Sherrod et al. (2000) reasoned that the most recent scarp-raising earthquake on the fault must have predated uplift of the lowest terrace. But on the basis of the trench stratigraphy and ^{14}C ages summarized here, we correlate the most recent earthquake on the fault with the 1050–1020 cal. yr B.P. earthquake that raised the terrace (Bucknam et al., 1992). The vertical fault displacement beneath the terrace during this most recent large earthquake either is too small to map ($<$0.3 m) or is expressed by broad warping of the terrace. Patterns of reverse-fault surface rupture during earthquakes of the past century include many irregular, discontinuous scarps no longer than the Toe Jam Hill fault scarp (Rubin, 1996; Kelson et al., 2001).

Magnitude

Estimates of prehistoric earthquake magnitude commonly rely on comparisons of inferred rupture length to empirical regressions of historic length vs. magnitude (e.g., Wells and Coppersmith, 1994). Because patterns of historic reverse-fault ruptures are complex and discontinuous, paleomagnitude estimates that rely on scarp length may underestimate past earthquake magnitudes (Rubin, 1996). Patterns of Holocene rupture in the Seattle fault zone are probably similarly complex, and the 2.6 km length of known Holocene rupture on the Toe Jam Hill fault is only a fraction of the rupture length during an earthquake. Another approach is to estimate prehistoric earthquake magnitudes from distributions of fault slip measured in trenches (Table 1; Hemphill-Haley and Weldon, 1999). Because fault slips of 1–2 m imply rupture lengths of tens of kilometers (Wells and Coppersmith, 1994), the Toe Jam Hill fault trenches span, at most, 5% of the probable surface rupture length during earthquakes on the Seattle fault. Total displacement during individual earthquakes can be assigned to only two of the three or four earthquakes (C and D) in two trenches (Mossy Lane and Crane Lake; Fig. 6). Using a sample of two with the methods of Hemphill-Haley and Weldon (1999) yields paleomagnitude estimates—M_w = 7.0 for earthquake C and M_w = 7.2 for earthquake D—with large uncertainties (–0.3, +0.8 M). Worldwide magnitude-displacement regressions give magnitudes ~0.3 M lower (Wells and Coppersmith, 1994). The higher estimate for earthquake D, which we correlate with the 1050–1020 cal. yr B.P. earthquake, is more consistent with the magnitude suggested by the earthquake's effects (Bucknam et al., 1992; Atwater and Moore, 1992; Schuster et al., 1992; Jacoby et al., 1992). Using the rupture-length vs. magnitude regressions of Wells and Coppersmith (1994) with the higher-magnitude estimates (without uncertainties) suggests 36–54 km and 52–80 km lengths of surface rupture during earthquakes C and D, respectively. Such long ruptures are inconsistent with earthquake rupture on the Toe Jam Hill backthrust independent of slip on the Seattle fault.

CONCLUSIONS

Five trenches across the 1- to 6-m-high scarp of the Toe Jam Hill fault, a 2.6-km-long, north-dipping backthrust to the Seattle fault, yield the first ^{14}C-measured recurrence intervals for a crustal fault in western Washington. Folded and faulted strata, liquefaction features, and forest soil A horizons buried by hanging-wall-collapse colluvium record three, or possibly four earthquakes, between 2.5 ka and 1.0 ka. The most recent earthquake is probably the 1050–1020 cal. yr B.P. earthquake, which raised marine terraces and triggered a tsunami in Puget Sound. Imprecisely dated evidence of older earthquakes elsewhere in Puget Sound may correlate with other Toe Jam Hill fault earthquakes. Surface folding and faulting of ~1–2 m per earthquake, estimated from stratigraphic and surface offsets, suggest late Holocene earthquake magnitudes near M = 7, corresponding with surface ruptures of >36 km. Surface deformation associated with less well understood late Pleistocene earthquakes suggests that they were smaller than late Holocene earthquakes. Postglacial (since 16 ka) recurrence intervals for the Toe Jam Hill fault range from 12,000 yr between late Pleistocene and late Holocene earthquakes to as little as a century or less between late Holocene earthquakes. Corresponding slip rates are ~0.2 mm/yr for the postglacial and ~2 mm/yr for the late Holocene displacements, compared with postglacial estimates for the Seattle fault zone of ~1 mm/yr. The earthquake history of the Toe Jam Hill fault is at least a partial proxy for the earthquake history of the Seattle fault and other faults in the Seattle fault zone.

ACKNOWLEDGMENTS

Supported by the Earthquake Hazards Program of the U.S. Geological Survey. The guidance and enthusiasm of Bill Laprade were invaluable, as were ^{14}C analyses provided by the National Ocean Sciences AMS Facility, Woods Hole Oceanographic Institution; Geochron Laboratories, Inc., Cambridge, Massachusetts; Lawrence Livermore National Laboratories, Livermore, California; and Beta Analytic, Inc., Miami, Florida. Land access and logistical support provided by Port Blakely Tree Farms, L.P., through the tireless efforts of Scott Sheldon, made the study possible. Pat Cearley of Burley, Washington, expertly excavated the trenches and, along with Jon Dueker, guided us in site restoration. Unsung trench loggers include John Cox, Ralph Haugerud, Charles Narwold, Bill Laprade, and Mark Molinari. Derek Booth and Kathy Troost took an early interest in our work and helped interpret glacial sediments. Estella Leopold analyzed pollen samples. Bob Bucknam's shoreline studies led to discovery of the Toe Jam Hill fault scarp, which was first pointed out by Gerry Elfendahl on ALSM imagery provided by Kitsap County Public Utilities District No. 1. Insightful reviews by Carol Prentice, Liz Schermer, Jim McCalpin, and Bob Karlin prodded us to improve the paper.

REFERENCES CITED

Atwater, B.F., 1999, Radiocarbon dating of a Seattle earthquake to A.D. 900–930 [abs.]: Seismological Research Letters, v. 70, p. 232.

Atwater, B.F., and Moore, A.L., 1992, A tsunami about 1000 years ago in Puget Sound, Washington: Science, v. 258, p. 1614–1617.

Bilham, R., and Yu, T.-T., 2000, The morphology of thrust faulting in the 21 September 1999, Chichi, Taiwan earthquake: Journal of Asian Science, v. 18, p. 351–367.

Birkeland, P.W., 1999, Soils and geomorphology: New York, Oxford University Press, 430 p.

Blakely, R.J., Wells, R.E., Weaver, C.S., and Johnson, S.Y., 2002, Location, structure, and seismicity of the Seattle fault zone, Washington: Evidence from aeromagnetic anomalies, geologic mapping, and seismic-reflection data: Geological Society of America Bulletin, v. 114, p. 169–177.

Bourgeois, J., and Johnson, S.Y., 2001, Geologic evidence of earthquakes at the Snohomish delta, Washington, in the past 1200 years: Geological Society of America Bulletin, v. 113, p. 482–494.

Brocher, T.M., Parsons, T., Blakely, R.J., Christensen, N.I., Fisher, M.A., Wells, R.E., andthe SHIPS Working Group, 2001, Upper crustal structure in Puget Lowland, Washington—Results from the 1998 seismic hazards investigation in Puget Sound: Journal of Geophysical Research, v. 106, p. 13,541–13,564.

Bronk Ramsey, C., 1998, Probability and dating: Radiocarbon, v. 40, p. 461–474.

Bucknam, R.C., Hemphill-Haley, E., and Leopold, E.B., 1992, Abrupt uplift within the past 1,700 years at southern Puget Sound, Washington: Science, v. 258,

p. 1611–1614.
Bucknam, R.C., Sherrod, B.L., and Elfendahl, G., 1999, A fault scarp of probable Holocene age in the Seattle fault zone, Bainbridge Island, Washington: Seismological Research Letters, v. 258, p. 1611–1614.
Calvert, A.J., Fisher, M.A., andSHIPS Working Group, 2001, Imaging the Seattle fault zone with high-resolution seismic tomography: Geophysical Research Letters, v. 28, p. 2337–2340.
Dethier, D.P., 1988, The soil chronosequence along the Cowlitz River, Washington, *in* Harden, J.W., ed., Soil chronosequences in the western United States: U.S. Geological Survey Bulletin 1590-F, p. F1–F47.
Dolan, J.F., Sieh, K., Rockwell, T.K., Yeats, R.S., Shaw, J., Suppe, J., Huftile, G., and Gath, E., 1995, Prospects for larger or more frequent earthquakes in greater metropolitan Los Angeles, California: Science, v. 267, p. 199–205.
Frankel, A.D., Petersen, M.D., Mueller, C.S., Haller, K.M., Wheeler, R.L., Leyendecker, E.V., Wesson, R.L., Harmsen, S.C., Cramer, C.H., Perkins, D.M., and Rukstales, K.S., 2002, Documentation for the 2002 update of the National Seismic Hazard Maps: U.S. Geological Survey Open-File Report 02–420, version 1.0, scale 1:7,000,000 (download at http://pubs.usgs.gov/of/2002/ofr-02-420/).
Garcia, A.F., 1996, Active tectonic deformation and late Pleistocene and Holocene geomorphic and soil profile evolution in the Dosewallips River drainage basin, Olympic Mountains, western Washington State [M.S.thesis]: Albuquerque, University of New Mexico, 152 p.
Gavin, D.G., 2000, Holocene fire history of a coastal temperate rain forest, Vancouver Island, British Columbia [Ph.D.thesis]: Seattle, University of Washington, 133 p.
Gavin, D.G., 2001, Estimation of inbuilt age in radiocarbon ages of soil charcoal for fire history studies: Radiocarbon, v. 43, p. 27–44.
Gower, H.D., Yount, J.C., and Crosson, R.S., 1985, Seismotectonic map of the Puget Sound region, Washington: U.S. Geological Survey Map I-1613, scale 1: 250,000.
Haeussler, P.J., Wells, R.E., Blakely, R.J., Murphy, J., and Wooden, J.L., 2000, Structure and timing of movement on the Seattle fault at Green and Gold Mountains, Kitsap Peninsula, Washington: Geological Society of America Abstracts with Programs, v. 32, no. 6, p. A-16.
Harding, D.J., and Berghoff, G.S., 2000, Fault scarp detection beneath dense vegetation cover—Airborne laser mapping of the Seattle fault zone, Bainbridge Island, Washington State: Bethesda, Maryland, American Society of Photogrammetry and Remote Sensing, Proceedings, Annual Conference, 9 p. (on CD).
Harding, D.J., Johnson, S.Y., and Haugerud, R.A., 2002, Folding and rupture of an uplifted Holocene marine platform in the Seattle fault zone, Washington, revealed by airborne laser swath mapping: Geological Society of America Abstracts with Programs, v. 34, no. 5, p. A-107.
Haugerud, R.A., Harding, D.J., Johnson, S.Y., Harless, J.L., and Weaver, C.S., 2003, High-resolution lidar topography of the Puget Lowland—A bonanza for earth science: GSA Today, v. 13, no. 6, p. 4–10.
Hemphill-Haley, M.A., and Weldon, R.J., II, 1999, Estimating prehistoric earthquake magnitude from point measurements of surface rupture: Seismological Society of America Bulletin, v. 89, p. 1264–1279.
Hemstrom, M.A., and Franklin, J.F., 1982, Fire and other disturbances at Mt. Rainier National Park: Quaternary Research, v. 18, p. 32–51.
Hyndman, R.D., Mazzotti, S., Weichert, D., and Rogers, G.C., 2003, Frequency of large crustal earthquakes in Puget Sound–southern Georgia Strait predicted from geodetic and geologic deformation rates: Journal of Geophysical Research, v. 108, no. B1, citation no. 2033, DOI:10. 1029/2001JB001710.
Jacoby, G.C., Williams, P.L., and Buckley, B.M., 1992, Tree ring correlation between prehistoric landslides and abrupt tectonic events in Seattle, Washington: Science, v. 258, p. 1621–1623.
Johnson, S.Y., Potter, C.J., and Armentrout, J.M., 1994, Origin and evolution of the Seattle fault and Seattle basin: Geology, v. 22, p. 71–74 and oversize insert.
Johnson, S.Y., Dadisman, S.V., Childs, J.R., and Stanley, W.D., 1999, Active tectonics of the Seattle fault and central Puget Lowland—Implications for earthquake hazards: Geological Society of America Bulletin, v. 111, p. 1042–1053 and oversize insert.
Karlin, R.E., and Abella, S.E.B., 1996, A history of Pacific Northwest earthquakes recorded in Holocene sediments from Lake Washington: Journal of Geophysical Research, v. 101, p. 6137–6150.
Kelsey, H.M., Hull, A.G., Cashman, S.M., Berryman, K.R., Cashman, P.H., Trexler, J.H., Jr., and Begg, J.G., 1998, Paleoseismology of an active reverse fault in a forearc setting: The Poukawa fault zone, Hikurangi forearc, New Zealand: Geological Society of America Bulletin, v. 110, p. 1123–1148.
Kelson, K.I., Kang, K.-H., Page, W.D., Lee, C.-T., and Cluff, L.S., 2001, Representative styles of deformation along the Chelungpu fault from the 1999 Chi-Chi (Taiwan) earthquake: Geomorphic characteristics and responses of man-made structures: Seismological Society of America Bulletin, v. 91, p. 930–952.
Mazzotti, S., Dragert, H., Hyndman, R.D., Miller, M.M., and Henton, J.A., 2002, GPS deformation in a region of high crustal seismicity: North Cascadia forearc: Earth and Planetary Science Letters, v. 198, p. 41–48.
McCalpin, J.P., 1996, Paleoseismology: Orlando, Florida, Academic Press, 588 p.
McClay, K.R., 1992, Glossary of thrust tectonic terms, *in* McClay, K.R., ed., Thrust tectonics: London, Chapman and Hall, p. 418–433.
Miller, M.M., Miller, D.J., Rubin, C.M., Dragert, H., Wang, K., Qamar, A., and Goldfinger, C., 2001, GPS-determination of along-strike variation in Cascadia margin kinematics—Implications for relative plate motion, subduction zone coupling, and permanent deformation: Tectonics, v. 20, p. 161–176.
Nelson, A.R., Johnson, S.Y., Wells, R.E., Pezzopane, S.K., Kelsey, H.M., Sherrod, B.L., Bradley, L.-A., Koehler, R.D., III, Bucknam, R.C., Haugerud, R.A., and LaPrade, W.T., 2002, Field and laboratory data from an earthquake history study of the Toe Jam Hill fault, Bainbridge Island, Washington: U.S. Geological Survey Open-File Report 02–60, 2 plates and 37 p. (download at http://pubs.usgs.gov/of/2002/ofr-02–0060/).
Ota, Y., Watanabe, M., Suzuki, Y., and Sawa, H., 2003, Geomorphological identification of pre-existing Chelungpu active fault in central Taiwan, especially on its relation to the location of the surface rupture of the 1999 Chichi earthquake: Quaternary International (in press).
Philip, H., Rogozhin, E., Cisternas, A., Bousquet, J.C., Borisov, B., and Karakhanian, A., 1992, The Armenian earthquake of 1988 December 7: Faulting and folding, neotectonics and palaeoseismicity: Geophysical Journal International, v. 110, p. 141–158.
Porter, S.C., and Swanson, T.W., 1998, Radiocarbon age constraints on rates of advance and retreat of the Puget Lobe of the Cordilleran ice sheet during the last glaciation: Quaternary Research, v. 50, no. 3, p. 205–213.
Pratt, T.L., Johnson, S.Y., Potter, C.J., and Stephenson, W., 1997, Seismic reflection images beneath Puget Sound, western Washington State: The Puget Lowland thrust sheet hypothesis: Journal of Geophysical Research, v. 102, p. 27,469–27,490.
Rubin, C.M., 1996, Systematic underestimation of earthquake magnitudes from large intracontinental reverse faults: Historical ruptures break across segment boundaries: Geology, v. 24, p. 989–992.
Schuster, R.L., Logan, R.L., and Pringle, P.T., 1992, Prehistoric rock avalanches in the Olympic Mountains, Washington: Science, v. 258, p. 1620–1623.
Sherrod, B.L., 2001, Evidence for earthquake-induced subsidence about 1100 yr ago in coastal marshes of southern Puget Sound, Washington: Geological Society of America Bulletin, v. 113, p. 1299–1311.
Sherrod, B.L., 2002, Late Quaternary surface rupture along the Seattle fault zone near Bellevue, Washington: Eos (Transactions, American Geophysical Union), v. 83, abstract S21C-12.
Sherrod, B.L., Bucknam, R.C., and Leopold, E.B., 2000, Holocene relative sea-level changes along the Seattle fault at Restoration Point, Washington: Quaternary Research, v. 54, p. 384–393.
Stuiver, M., Reimer, P.J., Bard, E., Beck, J.W., Burr, G.S., Hughen, K.A., Kromer, B., McCormac, G., von der Plicht, J., and Spurk, M., 1998, INTCAL98 radiocarbon age calibration, 24,000-0 cal. B.P.: Radiocarbon, v. 40, p. 1041–1084.
Sugiyama, Y., 2000, Research on earthquake potential evaluation by active faults: Geological Survey of Japan Bulletin, v. 51, no. 9, p. 379–389.
ten Brink, U.S., Molzer, P.C., Fisher, M.A., Blakely, R.J., Bucknam, R.C., Parsons, T., Crosson, R.S., and Creager, K.C., 2002, Subsurface geometry and evolution of the Seattle fault zone and the Seattle basin, Washington: Seismological Society of America Bulletin, v. 92, p. 1737–1753.
Thorson, R.M., 1996, Earthquake recurrence and glacial loading in western Washington: Geological Society of America Bulletin, v. 108, p. 1182–1191.
Thorson, R.M., 2000a, Shoreline stratigraphy of Lake Washington: Implications for Holocene crustal strain and earthquake recurrence in the Cascadia forearc, *in* Clague, J.J., Atwater, B.F., Wang, K., Wang, Y., and Wong, I., compilers, Penrose Conference 2000, Great Cascadia Earthquake Tricentennial, Program Summary and Abstracts: Oregon Department of Geology and Mineral Industries Special Paper 33, p. 120–121.
Thorson, R.M., 2000b, Glacial tectonics: A deeper perspective: Quaternary Science Reviews, v. 19, p. 1391–1398.
Wells, D., and Coppersmith, K.J., 1994, New empirical relationships among magnitude, rupture length, rupture width, rupture area, and surface displacement: Seismological Society of America Bulletin, v. 84, p. 974–1002.
Wells, R.E., Weaver, C.S., and Blakely, R.J., 1998, Forearc migration in Cascadia and its neotectonic significance: Geology, v. 26, p. 759–762.
Wilson, J.R., Bartholomew, M.J., and Carson, R.J., 1979, Late Quaternary faults and their relationship to tectonism in the Olympic Peninsula, Washington: Geology, v. 7, p. 235–239.
Zdanowicz, C.M., Zielinski, G.A., and Germani, M.S., 1999, Mount Mazama eruption: Calendrical age verified and atmospheric impact assessed: Geology, v. 27, p. 621–624.

MANUSCRIPT RECEIVED BY THE SOCIETY 20 SEPTEMBER 2002
REVISED MANUSCRIPT RECEIVED 27 MAY 2003
MANUSCRIPT ACCEPTED 10 JUNE 2003

Printed in the USA